

## DISCLAIMER

This report was prepared as an account of work sponsored by an agency of the United States Government. Neither the United States Government nor any agency thereof, nor any of their employees, makes any warranty, express or implied, or assumes any legal liability or responsibility for the accuracy, completeness, or usefulness of any information, apparatus, product, or process disclosed, or represents that its use would not infringe privately owned rights. Reference herein to any specific commercial product, process, or service by trade name, trademark, manufacturer, or otherwise does not necessarily constitute or imply its endorsement, recommendation, or favoring by the United States Government or any agency thereof. The views and opinions of authors expressed herein do not necessarily state or reflect those of the United States Government or any agency thereof.

ANL/NDM-83

### THE FISSION CROSS SECTIONS OF SOME THORIUM, URANIUM, NEPTUNIUM AND PLUTONIUM ISOTOPES RELATIVE TO $^{235}\text{U}$

by

J. W. Meadows

October, 1983

ANL/NDM--83

DE84 003214

NUCLEAR REACTIONS  $^{230}\text{Th}$ ,  $^{232}\text{Th}$ ,  $^{233}\text{U}$ ,  $^{234}\text{U}$ ,  $^{236}\text{U}$ ,  $^{238}\text{U}$ ,  
 $^{237}\text{Np}$ ,  $^{239}\text{Pu}$ ,  $^{240}\text{Pu}$ ,  $^{242}\text{Pu(n,f)}$ ,  $E = 0.1$  to  $10$  MeV;  
measured ratio  $\sigma(E)$  relative to  $^{235}\text{U}$ .

\* This work supported by the U.S. Department of Energy

Applied Physics Division  
Argonne National Laboratory  
9700 South Cass Avenue  
Argonne, Illinois 60439

#### NOTICE

**PORTIONS OF THIS REPORT ARE ILLEGIBLE.**

It has been reproduced from the best  
available copy to permit the broadest  
possible availability.

DISTRIBUTION OF THIS DOCUMENT IS UNLIMITED

Seb

## **DISCLAIMER**

**This report was prepared as an account of work sponsored by an agency of the United States Government. Neither the United States Government nor any agency Thereof, nor any of their employees, makes any warranty, express or implied, or assumes any legal liability or responsibility for the accuracy, completeness, or usefulness of any information, apparatus, product, or process disclosed, or represents that its use would not infringe privately owned rights. Reference herein to any specific commercial product, process, or service by trade name, trademark, manufacturer, or otherwise does not necessarily constitute or imply its endorsement, recommendation, or favoring by the United States Government or any agency thereof. The views and opinions of authors expressed herein do not necessarily state or reflect those of the United States Government or any agency thereof.**

## **DISCLAIMER**

**Portions of this document may be illegible in electronic image products. Images are produced from the best available original document.**

## NUCLEAR DATA AND MEASUREMENTS SERIES

The Nuclear Data and Measurements Series presents results of studies in the field of microscopic nuclear data. The primary objective is the dissemination of information in the comprehensive form required for nuclear technology applications. This Series is devoted to: a) measured microscopic nuclear parameters, b) experimental techniques and facilities employed in measurements, c) the analysis, correlation and interpretation of nuclear data, and d) the evaluation of nuclear data. Contributions to this Series are reviewed to assure technical competence and, unless otherwise stated, the contents can be formally referenced. This Series does not supplant formal journal publication but it does provide the more extensive information required for technological applications (e.g., tabulated numerical data) in a timely manner.

INFORMATION ABOUT OTHER ISSUES IN THE ANL/NDM SERIES:

A list of titles and authors for reports ANL/NDM-1 through ANL/NDM-50 can be obtained by referring to any report of this series numbered ANL/NDM-51 through ANL/NDM-76. Requests for a complete list of titles or for copies of previous reports should be directed to:

Section Secretary  
Applied Nuclear Physics Section  
Applied Physics Division  
Building 316  
Argonne National Laboratory  
9700 South Cass Avenue  
Argonne, Illinois 60439  
USA

ANL/NDM-51 Measured and Evaluated Neutron Cross Sections of Elemental Bismuth by A. Smith, P. Guenther, D. Smith and J. Whalen, April 1980.

ANL/NDM-52 Neutron Total and Scattering Cross Sections of  $^6\text{Li}$  in the Few MeV Region by P. Guenther, A. Smith and J. Whalen, February 1980.

ANL/NDM-53 Neutron Source Investigations in Support of the Cross Section Program at the Argonne Fast-Neutron Generator by James W. Meadows and Donald L. Smith, May 1980.

ANL/NDM-54 The Nonelastic-Scattering Cross Sections of Elemental Nickel by A. B. Smith, P. T. Guenther and J. F. Whalen, June 1980.

ANL/NDM-55 Thermal Neutron Calibration of a Tritium Extraction Facility using the  $^6\text{Li}(\text{n},\text{t})^4\text{He}/^{197}\text{Au}(\text{n},\gamma)^{198}\text{Au}$  Cross Section Ratio for Standardization by M. M. Bretscher and D. L. Smith, August 1980.

ANL/NDM-56 Fast-Neutron Interactions with  $^{182}\text{W}$ ,  $^{184}\text{W}$  and  $^{186}\text{W}$  by P. T. Guenther, A. B. Smith and J. F. Whalen, December 1980.

ANL/NDM-57 The Total, Elastic- and Inelastic-Scattering Fast-Neutron Cross Sections of Natural Chromium by Peter T. Guenther, Alan B. Smith and James F. Whalen, January 1981.

ANL/NDM-58 Review of Measurement Techniques for the Neutron Capture Process by W. P. Poenitz, August 1981.

ANL/NDM-59 Review of the Importance of the Neutron Capture Process in Fission Reactors by Wolfgang P. Poenitz, July 1981.

ANL/NDM-60 Neutron Capture Activation Cross Sections of  $^{94}\text{Zr}$ ,  $^{96}\text{Zr}$ ,  $^{98}\text{Mo}$ , and  $^{110},^{114},^{116}\text{Cd}$  at Thermal and 30 keV Energy by John M. Wyrick and Wolfgang P. Poenitz, (to be published).

ANL/NDM-61 Fast-neutron Total and Scattering Cross Sections of  $^{58}\text{Ni}$  by Carl Budtz-Jørgensen, Peter T. Guenther, Alan B. Smith and James F. Whalen, September 1981.

ANL/NDM-62 Covariance Matrices and Applications to the Field of Nuclear Data by Donald L. Smith, November 1981.

ANL/NDM-63 On Neutron Inelastic-Scattering Cross Sections of  $^{232}\text{Th}$ ,  $^{233}\text{U}$ ,  $^{235}\text{U}$ ,  $^{238}\text{U}$ ,  $^{239}\text{U}$ , and  $^{239}\text{Pu}$  and  $^{240}\text{Pu}$  by Alan B. Smith and Peter T. Guenther, January 1982.

ANL/NDM-64 The Fission-Fragment Angular Distributions and Total Kinetic Energies for  $^{235}\text{U}(\text{n},\text{f})$  from 0.18 to 8.83 MeV by James W. Meadows and Carl Budtz-Jørgensen, January 1982.

ANL/NDM-65 Note on the Elastic Scattering of Several-MeV Neutrons from Elemental Calcium by Alan B. Smith and Peter T. Guenther, March 1982.

ANL/NDM-66 Fast-neutron Scattering Cross Sections of Elemental Silver by Alan B. Smith and Peter T. Guenther, May 1982.

ANL/NDM-67 Non-evaluation Applications for Covariance Matrices by Donald L. Smith, July 1982.

ANL/NDM-68 Fast-neutron Total and Scattering Cross Sections of  $^{103}\text{Rh}$  by Alan B. Smith, Peter T. Guenther and James F. Whalen, July 1982.

ANL/NDM-69 Fast-neutron Scattering Cross Sections of Elemental Zirconium by Alan B. Smith and Peter T. Guenther, December 1982.

ANL/NDM-70 Fast-neutron Total and Scattering Cross Sections of Niobium by Alan B. Smith, Peter T. Guenther and James F. Whalen, July 1982.

ANL/NDM-71 Fast-neutron Total and Scattering Cross Sections of Elemental Palladium by Alan B. Smith, Peter T. Guenther and James F. Whalen, June 1982.

ANL/NDM-72 Fast-neutron Scattering from Elemental Cadmium by Alan B. Smith and Peter T. Guenther, July 1982.

ANL/NDM-73 Fast-neutron Elastic-Scattering Cross Sections of Elemental Tin by C. Budtz-Jørgensen, Peter T. Guenther and Alan B. Smith, July 1982.

ANL/NDM-74 Evaluation of the  $^{238}\text{U}$  Neutron Total Cross Section by Wolfgang Poenitz, Alan B. Smith and Robert Howerton, December 1982.

ANL/NDM-75 Neutron Total and Scattering Cross Sections of Elemental Antimony  
by Alan B. Smith, Peter T. Guenther and James F. Whalen,  
September 1982.

ANL/NDM-76 Scattering of Fast-Neutrons from Elemental Molybdenum  
by Alan B. Smith and Peter T. Guenther, November 1982.

ANL/NDM-77 A Least-Squares Method for Deriving Reaction Differential  
Cross Section Information from Measurements Performed in  
Diverse Neutron Fields by Donald L. Smith, November 1982.

ANL/NDM-78 Fast-Neutron Total and Elastic-Scattering Cross Sections  
of Elemental Indium by A. B. Smith, P. T. Guenther, and  
J. F. Whalen, November 1982.

ANL/NDM-79 Few-MeV Neutrons Incident on Yttrium by C. Budtz-Jørgensen,  
P. Guenther, A. Smith and J. Whalen, June 1983.

ANL/NDM-80 Neutron Total Cross Section Measurements in the Energy Region  
from 47 keV to 20 MeV by W. P. Poenitz and J. F. Whalen,  
July 1983.

ANL/NDM-81 Covariances for Neutron Cross Sections Calculated Using a  
Regional Model Based on Elemental-Model Fits to Experimental  
Data by Donald L. Smith and Peter T. Guenther, (to be published).

ANL/NDM-82 Reaction Differential Cross Sections from the Least-Squares  
Unfolding of Ratio Data Measured in Diverse Neutron Fields  
by D. L. Smith (to be published).

	<u>Page</u>
Abstract . . . . .	ix
I. Introduction . . . . .	1
II. Experimental Methods, Procedures and Apparatus . . . . .	1
II.1. The basic Experimental Method . . . . .	1
II.2. The Experimental Apparatus . . . . .	3
II.2.1. The Neutron Source . . . . .	3
II.2.2. The Fission Detector and Electronics . . . . .	4
II.2.3. Alpha Counting . . . . .	5
II.2.4. The Thermal Ratio Measurements . . . . .	5
II.2.5. Neutron Energies and Resolution . . . . .	6
II.3. Samples. . . . .	6
II.3.1. Sample Preparation . . . . .	6
II.3.2. Sample Assay . . . . .	7
1. Isotopic Dilution . . . . .	7
2. Colorimetric Analyses . . . . .	7
3. Calculated Specific Activity . . . . .	7
4. Measured Specific Activity . . . . .	7
5. Common Alpha Emitter . . . . .	8
6. Thermal Fission Ratio. . . . .	8
7. Thermal Fission Ratios with a Common Isotope . . . . .	9
8. Sample Intercomparison . . . . .	9
II.4. Correction to the Data . . . . .	10
II.4.1. Backgrounds . . . . .	10
II.4.2. Extrapolation to Zero Bias . . . . .	10
II.4.3. Scattered Neutrons . . . . .	10
II.4.4. Deposit Thickness, Momentum Transfer and Fragment Angular Distribution . . . . .	11

	<u>Page</u>
II.4.5. Isotopic Impurities and Neutron Spectrum . . . . .	12
III. Errors . . . . .	12
1. Half-lives . . . . .	12
2. Thermal Fission Cross Sections . . . . .	13
3. Isotopic Analyses. . . . .	13
4. Isotopic Dilution Analysis . . . . .	13
5. Colorimetric Analysis. . . . .	13
6. Alpha Count (Systematic) . . . . .	13
7. Thickness Correction . . . . .	13
8. Extrapolation. . . . .	14
9. Dead Time Correction . . . . .	14
10. Scattering Correction . . . . .	14
11. Counting Statistics . . . . .	14
12. Neutron Spectrum . . . . .	14
13. Neutron Energy . . . . .	14
14. Uncorrelated Error . . . . .	15
IV. Results and Discussion . . . . .	15
V. Summary. . . . .	16
VI. References . . . . .	17

## Tables

Table I. The Isotopic Analyses and Masses of the Uranium Samples.

Table II. Isotopic Analyses and Masses of the Thorium and Neptunium Samples.

Table III. The Isotopic Compositions and Masses of the Plutonium Samples.

Table IV. The Half-Lives and Thermal Fission Cross Sections Used in the Measurements.

Table V. The Average Fission Cross Section Ratios at the Normalization Energies Classified According to the Assay Method.

Table VI. The Various Sources of Error Contributing to the Total Error in Normalization.

Table VII. The Error in the Fission Cross Section Ratios Due to the Secondary Source Reactions.

Table VIII. The  $^{230}\text{Th}/^{235}\text{U}$  Fission Cross Section Ratios and the Resultant  $^{230}\text{Th}$  Fission Cross Sections.

Table IX. The  $^{232}\text{Th}/^{235}\text{U}$  Fission Cross Section Ratios and the Resultant  $^{232}\text{Th}$  Fission Cross Sections.

Table X. The  $^{233}\text{U}/^{235}\text{U}$  Fission Cross Section Ratios and the Resultant  $^{233}\text{Th}$  Fission Cross Sections.

Table XI. The  $^{234}\text{U}/^{235}\text{U}$  Fission Cross Section Ratios and the Resultant  $^{234}\text{Th}$  Fission Cross Sections.

Table XII. The  $^{236}\text{U}/^{235}\text{U}$  Fission Cross Section Ratios and the Resultant  $^{236}\text{Th}$  Fission Cross Sections.

Table XIII. The  $^{238}\text{U}/^{235}\text{U}$  Fission Cross Section Ratios and the Resultant  $^{238}\text{Th}$  Fission Cross Sections.

Table XIV. The  $^{237}\text{Np}/^{235}\text{U}$  Fission Cross Section Ratios and the Resultant  $^{237}\text{Th}$  Fission Cross Sections.

Table XV. The  $^{239}\text{Pu}/^{235}\text{U}$  Fission Cross Section Ratios and the Resultant  $^{239}\text{Th}$  Fission Cross Sections.

Table XVI. The  $^{240}\text{Pu}/^{235}\text{U}$  Fission Cross Section Ratios and the Resultant  $^{240}\text{Th}$  Fission Cross Sections.

Table XVII. The  $^{242}\text{Pu}/^{235}\text{U}$  Fission Cross Section Ratios and the Resultant  $^{242}\text{Th}$  Fission Cross Sections.

Table XVIII. The Effect of Changes in Secondary Data on the Fission Cross Section Ratio.

Table XIX. The Percentage Change in the Normalization of the Revised Fission Cross Section Ratios.

THE FISSION CROSS SECTIONS OF SOME THORIUM,  
URANIUM, NEPTUNIUM AND PLUTONIUM ISOTOPES  
RELATIVE TO  $^{235}\text{U}$

by

J. W. Meadows

Applied Physics Division

Argonne National Laboratory  
Argonne, Illinois 60439

ABSTRACT

Earlier results from the measurements, at this Laboratory, of the fission cross sections of  $^{230}\text{Th}$ ,  $^{232}\text{Th}$ ,  $^{233}\text{U}$ ,  $^{234}\text{U}$ ,  $^{236}\text{U}$ ,  $^{238}\text{U}$ ,  $^{237}\text{Np}$ ,  $^{239}\text{Pu}$ ,  $^{240}\text{Pu}$ , and  $^{242}\text{Pu}$  relative to  $^{235}\text{U}$  are reviewed with revisions to include changes in data processing procedures, alpha half lives and thermal fission cross sections. Some new data have also been included. The current experimental methods and procedures and the sample assay methods are described in detail and the sources of error are presented in a systematic manner.

---

\* This work supported by the U.S. Department of Energy.

## I. Introduction

For several years there has been an on-going program at the Argonne Fast Neutron Generator (FNG) Laboratory with the goal of measuring the fast neutron fission cross sections of the longer-lived fissionable isotopes relative to  $^{235}\text{U}$ , with accuracies of 1-2%. Results have been reported for  $^{230}\text{Th}$ ,  $^{232}\text{Th}$ ,  $^{233}\text{U}$ ,  $^{234}\text{U}$ ,  $^{236}\text{U}$ ,  $^{238}\text{U}$ ,  $^{237}\text{Np}$ ,  $^{239}\text{Pu}$ ,  $^{240}\text{Pu}$ , and  $^{242}\text{Pu}$ .<sup>1-10</sup> This list now includes all the measurements that were planned when the program was begun, and it is therefore appropriate to review and re-evaluate the data and make any indicated revisions in the results.

There has been no essential change in the approach used to obtain the data and the experimental rationale, procedures, methods and types of equipment have remained essentially the same throughout the work. Still, the passage of time, the accumulation of data and experience, and the increased availability of computing equipment has resulted in some degree of evolutionary change in the process whereby the raw data are converted to fission cross section ratios. In the earliest reports (particularly the  $^{238}\text{U}$  and  $^{233}\text{U}$  measurements<sup>1,2</sup>) some of the correction factors were based on very rough approximations; now these factors are derived from more precise and detailed calculations. The experimental foundation for other factors has been improved. Many of the fission cross section ratios depend to some degree on secondary experimental quantities, such as alpha half-lives and thermal fission cross section ratios, and there have been significant changes in some of these quantities.

All the measurements have been reprocessed to the extent needed to include these changes. In several cases results from additional measurements have been included; some were originally made for other reasons, but one set ( $^{233}\text{U}$ ) was made specifically for this report. The question of errors has been re-examined and put on a more consistent basis. The effects of these revisions are generally small. There are noticeable changes in some of the results but the magnitudes are comparable with the expected error.

## II. Experimental Methods, Procedures and Apparatus

The topics discussed in this section are presented in some detail although all the material has been reported previously. In particular the basic experimental method and the apparatus are essentially the same as that described in ref. 1. However, the determination of some corrections, as well as some of the experimental procedures, have changed and these changes, along with the methods of preparation and assay of specific samples, are scattered throughout refs. 1-10. The material presented here refers to current practice and applies to the revised results although the earlier method may be referred to if the change causes a noticeable revision.

### II.1. The Basic Experimental Method

The idealized form of the present experimental method involves

placing two monoisotopic samples with accurately known masses in the same monoenergetic neutron flux and measuring their relative fission rates with perfect detectors. Then

$$\frac{F_2(E)}{F_1(E)} = \frac{N_2}{N_1} \frac{\sigma_2(E)}{\sigma_1(E)} \quad (1)$$

where subscript 1 refers to the unknown isotope, 2 refers to the reference isotope,  $F$  is the fission rate,  $N$  is the number of sample atoms and  $\sigma$  is the fission cross section at neutron energy  $E$ .

In practical measurements the samples are not isotopically pure and their compositions and the ratio of their masses need to be accurately known. They are placed back-to-back near a localized neutron source and perpendicular to the direction of most of the neutrons. The neutron flux comes primarily (but not entirely) from the source and is not monoenergetic, although its principal component does have a narrow energy spread. The flux through the two samples is not quite the same due to geometry and transmission effects, and the fission rate depends on the order of the sample placement. The observed fission rate ratio due to neutrons impinging directly on the sample is

$$\frac{F_{xf}(E) - B_x(E) + \beta_x}{F_{rb}(E) - B_r(E) + \beta_r} = \frac{N_x}{N_r} \frac{\sigma_2(E)}{\sigma_1(E)} \frac{G_f T_f}{G_b} \frac{L_{xf}(E)}{L_{rb}(E)} \frac{S_{xf}(E)}{S_{rb}(E)} \frac{C_x(E)}{C_r(E)} \quad (2)$$

where  $x$  Refers to the unknown sample whose principal component is isotope 2.

$r$  Refers to the reference sample whose principal component is isotope 1.

$B_x, B_r$  The background corrections.

$\beta_x, \beta_r$  Corrections for fissions lying below the discriminator level.

$f$  Refers to the sample in the forward or zero deg. position.

$b$  Refers to the sample in the backward or 180 deg. position.

$G_f, G_b$  Geometry factors. In the present measurement where sample diameters are equal, they are associated with position only.

$T_f$  Neutron transmission coefficient for the sample support plates.  $T_b$  is always 1.0.

$L_{xf}, L_{rb}$  Correction factors for sample thickness, momentum transfer and fission fragment angular distributions.

$s_{xf}$ ,  $s_{rb}$  Correction factors for neutrons scattered by the fission detector and the neutron source structure.

$c_x$ ,  $c_r$  Correction factor for the minor isotopes and the neutron spectrum.

Eq. (2) is written explicitly for the case where the  $x$  sample is in the zero deg. position and a similar expression can be written for the  $r$  sample in that position. Measurements are made for these two orientations and the results are averaged. If  $G_b/G_f$ ,  $T_f$  and the ratios of the other position dependent correction factors are very near 1.0 then the  $G$  and the  $T$  terms will cancel to first order. If the following definitions are used

$$\mathcal{F}(E) = F(E) - B(E) + \beta \quad (3)$$

$$L(E) = 1 + \mathcal{L}(E) \quad (4)$$

$$S(E) = 1 + s(E) \quad (5)$$

then the first order form of the average is

$$\left( \frac{\mathcal{F}_x}{\mathcal{F}_r} \right)_{av} = \frac{N_x}{N_r} \frac{\sigma_2}{\sigma_1} \frac{c_x}{c_r} \left( 1 + \frac{\mathcal{L}_{xf} - \mathcal{L}_{rb} + \mathcal{L}_{xb} - \mathcal{L}_{rf}}{2} + \frac{s_{xf} - s_{rb} + s_{xb} - s_{rf}}{2} \right) \quad (6)$$

The explicit energy dependence of some of the terms has been dropped for convenience.

The first order conditions are fairly well satisfied in the present measurement. For example,

$$G_b/G_f \approx 1.02$$

$$T_f > 0.98$$

$$|\mathcal{L}| < 0.025$$

$$0.08 > s > 0.02$$

$$|s_x - s_r| < 0.03$$

The fission cross section ratios were calculated using eq. (6). The determination of the several terms and correction factors is described in the following paragraphs of this section.

## II.2. The Experimental Apparatus

### II.2.1. The Neutron Source

Protons or deuterons were accelerated by the Argonne 8 MeV Tandem Dynamitron Accelerator to energies ranging from  $\sim 2$  to  $\sim 7.5$  MeV. Neutrons with energies  $< 5$  MeV were produced by the  $^7\text{Li}(p,n)^7\text{Be}$  reaction.

Targets were prepared by evaporating elemental metallic lithium onto a tantalum backing. Target thicknesses were  $\sim 200$  keV above 2 MeV neutron energy but were thinner at lower energies. (The target thickness is defined here as the energy loss by the proton in the lithium layer at the  $^7\text{Li}(\text{p},\text{n})^7\text{Be}$  threshold.) Neutrons with energies  $> 5$  MeV were produced by the  $\text{D}(\text{d},\text{n})^3\text{He}$  reaction using a thin-window gas target. The experimental set-up using this target is illustrated in Fig. 1 and additional details are given in ref. 11. The gas cell was 2 cm long and filled with deuterium at a pressure of 2 atmospheres. The charged particle energy was controlled by a 90-deg. analyzing magnet and slit feed-back system. A pulsed and bunched charged particle beam was used to produce a pulsed neutron source and fast timing techniques selected those fissions suitably correlated with the neutron burst. The pulse period was 500 ns and the neutron pulse widths were  $\sim 2$  ns.

### II.2.2. The Fission Detector and Electronics

The fission detector, shown schematically in Fig. 1, was a low-mass double-ionization chamber with the samples deposited on both sides of the common cathode. The chamber was a steel specimen container with a friction-fit lid. The walls were 0.25 mm thick. The electrodes were 0.25 mm or 0.13 mm thick stainless steel or molydenum. The chamber was operated as a flow counter using methane as the counter gas because of its high electron mobility. Most measurements were made with cathode-anode separations of  $\sim 0.6$  cm but separations as large as 1.6 cm were occasionally used. Voltage gradients were maintained at  $\sim 650$  volts/cm. The fast rise of the ion chamber current pulse was used to provide good timing characteristics and the height of the current pulse was a measure of the electron charge produced in the active volume. Good separation between the alphas and fissions was obtained by keeping the pulse widths small until the alphas were removed by bias levels or by gating. A good discussion of the principles of this type of ion-chamber operation is given by Budtz-Jørgensen and Knitter.<sup>12</sup>

The electronic systems were the same for both sides of the double ion chamber. Signals from the anodes went to charge sensitive pre-amplifiers, which were capable of fast rise-times, then to clipping amplifiers where they were differentiated twice; first by 93-ohm clipping cables 1.5 m long and second, by the 4 ns amplifier time constants. The amplifier outputs were divided and one part triggered fast leading-edge discriminators which provided the start signals for the time-to-pulse-height converters. The stop signal came from a beam-pulse sensor located near the accelerator target. The other part of the clipping amplifier output went to a biased amplifier where the bias levels could be set to reject a large fraction of the alphas, and then to a stretcher. The two time signals and the two pulse-height signals were routed into separate mixers and sent to the data storage computer along with tags identifying the detector. They were stored in two two-parameter arrays for later inspection when final windows and bias

levels were set. The electronics after the mixers were slow and subject to some dead-time losses. However, the signals were mixed at this point so the dead-time was the same for both detectors. The number of accidental coincidences as well as those few signals arriving without tags were stored and used to correct the data where necessary. Usually the fission rates were too low to require any significant corrections and a large number of counts in either of these two channels indicated a fault in the electronics. The system was capable of a time resolution of  $\sim 3$  ns but this required some sacrifice in beam current so many measurements were made with a time resolution  $\sim 5$  ns.

As the alpha rate approached  $10^6$  alphas/sec the alpha-fission separation deteriorated due to pile-up in the biased amplifier. The separation was improved when this unit was replaced by a fast linear gate and stretcher (E.G.&G. LG105/N) gated by a 45 ns pulse from the fast discriminator. Good results were obtained with  $\sim 300$   $\mu$ g  $^{240}\text{Pu}$  in the chamber.

#### II.2.3. Alpha Counting

Most of the alpha counting for mass determinations was done in a low geometry alpha counter that was constructed to tolerances of 0.005 mm. The counter aperture was 1.27 cm in diameter. The alphas were detected by a 2 cm diameter silicon detector with a resolution of  $\sim 30$  keV which was placed immediately behind the aperture. Sample distances depended on the sample holder used but typical values began at 4.57 cm and increased in multiples of 5.08 cm. In the course of these measurements the counter was taken apart several times for cleaning. After each re-assembly the critical dimensions were measured and its performance was confirmed by counting standard samples. Geometry factors were calculated by a Monte Carlo integration procedure<sup>13</sup> and also by a series expansion.<sup>14</sup>

The  $^{238}\text{U}$  samples were counted in a  $2\pi$  proportional counter (see method (4) in Section II.3.2.).

#### II.2.4. The Thermal Ratio Measurements

Many of the thermal fission ratio measurements were made in the thermal column of the Argonne Thermal Source Reactor (ATSR) at a point where the cadmium ratio for  $^{197}\text{Au}(n,\gamma)^{198}\text{Au}$  was  $\sim 500$ . Separate data collection systems were used for each detector, and since the count rates were often very different, a significant dead time correction was required. Other thermal ratio measurements were made at the FNG where the fission chamber was placed in the center of a stack of polyethylene blocks about 65 cm on a side. The FNG target produced neutrons by the  $^7\text{Li}(p,n)^7\text{Be}$  reaction with energies of 0.45 - 0.65 MeV and was located at the center of one face of the block. Cadmium ratios for  $^{235}\text{U}(n,f)$  were  $\sim 200$ . The detectors and electronics were the same as described in Section II.2.2, except the fast signal from the ion chamber was divided and one part sent through a 200 ns delay to

provide the stop pulse. Since the data collection rates were usually low and since the detector signals were mixed before any of the critical slow electronics were reached there was no dead time correction.

### II.2.5. Neutron Energies and Resolution

The calibration and tests of the FNG energy scale are described in ref. 15.

The energy is controlled by a 90-deg. analyzing magnet and slit feedback system that was calibrated by observing the thresholds of the  $^7\text{Li}(\text{p},\text{n})^7\text{Be}$  ( $1880.60 \pm .04$  keV)<sup>16</sup>,  $^{11}\text{B}(\text{p},\text{n})^{11}\text{C}$  ( $3016.4 \pm 1.6$  keV)<sup>17</sup> and  $^{27}\text{Al}(\text{p},\text{n})^{27}\text{Si}$  ( $5796.9 \pm 3.8$  keV)<sup>16</sup> reactions. The energy distributions of neutrons from the primary source reaction that were incident on the samples were calculated from the incident particle energy, the angular distribution of the source reaction, the lithium or gas target thickness and the source-sample geometry. The neutron energies listed in Tables VIII thru XVII are the averages of these distributions and the resolutions are their full-width at half-maximum. Energy losses in the lithium layer, the gas cell window and in the deuterium cell are based on information from ref. 18. The reaction Q values for the  $^7\text{Li}(\text{p},\text{n})^7\text{Be}$  and  $\text{D}(\text{d},\text{n})^3\text{He}$  reaction (-1.644 and 3.268 MeV) are those quoted by Liskien and Paulsen.<sup>19,20</sup>

### II.3. Samples

The samples used in these measurements, their isotopic analyses and their weights are listed in Tables I, II and III. Many have been referred to in earlier reports but their numbers have been slightly different. Samples 235 5-1 and 5-2 are listed as 51 and 52 refs. 6 and 7, the  $^{233}\text{U}$  samples 1002, 1202 and 1402 are listed as 10, 12 and 14 in ref. 2 and 235 SST-5 is listed as 235-5 in ref 6.

Several of the  $^{235}\text{U}$  samples (235 5-1, 5-2, SST-5, 13 and 3) were used in a number of the ratio measurements and, for this reason, are sometimes referred to as "standard" samples. Three of these (5-1, 5-2 and SST-5) were among those used in a series of measurements at this laboratory where reference  $^{235}\text{U}$  deposits from several laboratories were intercompared.<sup>21</sup> The sample weights in Table I do not quite match those of ref. 21 because they are based on a different value of the  $^{234}\text{U}$  half-life and a different set of alpha counts.

#### II.3.1. Sample Preparation

All samples were mounted on 0.25 mm thick stainless steel plates, 0.13 mm thick molybdenum plates, or 0.13 mm thick platinum plates. All the uranium samples with numbers starting with U-235 SST or U-238 Mo were prepared by vacuum evaporation of  $\text{UF}_4$ . All other uranium samples were prepared by molecular plating following a procedure developed by Parker et al.<sup>22</sup> They

were then all heated to the same temperature, which was not high enough for conversion to  $U_3O_8$ . They should all have the same composition but that composition is not known. The thorium samples were deposited on platinum by molecular plating followed by heating to  $\sim 750$  deg. C. The neptunium samples were deposited on platinum by electrodeposition, following a procedure described by Ko<sup>23</sup>, then heated to  $\sim 850$  deg. C. Some plutonium samples were deposited by molecular plating but electrodeposition was used for most of them. These were then heated to convert them to  $PuO_2$ .

The alpha spectra of all these samples were inspected, but no impurities of any significance were found. The  $^{233}U$  spectra did show members of the  $^{232}U$  decay chain; the  $^{237}Np$  spectra indicated a small amount of plutonium, but the amount was  $< 0.01$  atom%; the  $^{240}Pu$  samples contained a small amount of  $^{241}Am$  formed by the decay of  $^{241}Pu$  and that is included in the isotopic analyses.

### II.3.2. Sample Assay

As shown by eq. (6), the quantity of interest is the ratio of sample atoms,  $N_x/N_r$ . In some cases this can be measured directly; in others it is necessary to determine  $N$  for each individual sample. Where possible  $N_x/N_r$  was determined by two or more methods and the eight assay methods used are listed below. However, these are actually a variation of three basic techniques: i) destructive analysis (1,2), ii) alpha counting combined with specific activities (3,4,5,8) and iii) relative thermal fission rates (6,7).

(1) Isotopic Dilution. A sample was dissolved from its backing and the amount of material was measured by isotopic dilution. This method could not be used for neptunium as there was no suitable dilutant.

(2) Colorimetric Analyses. This was similar to (1) except the amount of material was measured by comparison to standard solutions using colorimetry. This procedure was used only for some of the  $^{235}U$  and  $^{238}U$  samples.

(3) Calculated Specific Activity. The specific activity of the sample material was calculated from the isotopic analyses and the half-lives listed in Tables I-IV. The amount of material present was then determined by low geometry alpha counting in a counter with well determined geometry factors. Material with a low alpha activity was often spiked with a small amount of a more active isotope to provide a convenient alpha decay rate.

(4) Measured Specific Activity. Samples were prepared from a particular batch of material and alpha counted. The amount of material was determined by (1) and/or (2). This gave the specific activity and the weight of any additional samples made from the same material was determined by alpha counting. These measurements were most readily made by low geometry alpha counting. However,  $2\pi$  counting was also usable if the specific activity

measurements covered a range of sample thicknesses so corrections could be made for self-absorption and back-scattering. The U-238 Mo-based samples were measured in this fashion.

(5) Common Alpha Emitter. This is a special case where the two samples contain a common isotope that supplies most of the alpha decay. The ratio of the decay rates is

$$\frac{C_x G_r}{C_r G_x} = \frac{N_x}{N_r} \frac{P_{xc}}{P_{rc}} \frac{1 + \frac{\tau_c}{P_{xc}} \sum_{i \neq c} P_{xi}/\tau_i}{1 + \frac{\tau_c}{P_{rc}} \sum_{i \neq c} P_{ri}/\tau_i} \quad (7)$$

where subscripts r and x refer to the unknown and reference samples, subscript c refers to the common isotope, C is the alpha count rate, G is the geometry factor,  $\tau$  is the half-life and P is the isotopic mole-fraction. In those cases where

$$\tau_c/P_c \ll \tau_i/P_i \quad i \neq c \quad (8)$$

the result is almost independent of any half-life measurements. If the samples have the same diameter and are mounted on similar backings then counted at the same position in the alpha counter, the geometry factors are also eliminated. Since the reference isotope in this measurement was always  $^{235}\text{U}$  this method could only be used for the uranium isotopes.

(6) Thermal Fission Ratio. This method assumes that the fission cross section ratios at thermal energies are accurately known. The relative fission rates of pairs of samples were measured at thermal energies and the thermal fission cross sections were used to determine  $N_x/N_r$ . Both samples must contain appreciable amounts of thermally fissionable isotopes. This is no problem for the r sample since the reference isotope is always  $^{235}\text{U}$  but it may be necessary to prepare a special mixture for the x sample. Equation (6) and the corrections of Section II.4.1 still apply. However at very low energies

$$B \rightarrow 0$$

$$S \rightarrow 1.0$$

$$L_{xf} \rightarrow L_{xb}$$

$$L_{rb} \rightarrow L_{rf}$$

and eq. (6) may be written in the form.

$$\left( \frac{F_x}{F_r} \right)_{av} = \frac{N_x L_x}{N_r L_r} \frac{P_{xt} \bar{\sigma}_t}{P_{rl} \bar{\sigma}_l} \frac{1 + (P_{xt} \bar{\sigma}_t)^{-1} \sum_{i \neq t} (P_{xi} \bar{\sigma}_i)}{1 + (P_{rl} \bar{\sigma}_l)^{-1} \sum_{i \neq l} (P_{ri} \bar{\sigma}_i)} \quad (7)$$

where t and l refers to the principle thermally fissionable isotope in the x and r samples,  $\bar{\sigma}$  is the fission cross section averaged over the thermal spectrum and all other terms are defined in Sections II.1 and II.2.5. If

$$P_x \bar{\sigma}_t \gg \sum_{i \neq t} (P_{xi} \bar{\sigma}_i) \quad (8)$$

the term in [] becomes a small correction and  $N_x/N_r$  depends on  $\bar{\sigma}_t/\bar{\sigma}_l$ .

(7) Thermal Fission Ratios with a Common Isotope. This is a special case of (6) and could be used only with  $^{234}\text{U}$ ,  $^{236}\text{U}$  and  $^{238}\text{U}$ . Some samples were prepared from material containing  $\sim 10\%$   $^{235}\text{U}$ . Since the fissionable isotope was  $^{235}\text{U}$  in both samples there was no dependence on the thermal fission cross sections.

(8) Sample Intercomparison. This was used only for some high purity samples where reliable specific activities could not be determined. The fission rates of these samples were compared with the fission rates of other samples whose masses had been determined by methods (3) and (4). Whenever this method is used in the ratio measurements it is listed under "Calculated Specific Activity" since the masses of most of the reference samples were measured by that method.

The alpha half-lives<sup>24-28</sup> and thermal fission cross sections used are listed in Table IV and the ones that are of particular importance are indicated. The  $^{233}\text{U}$ ,  $^{235}\text{U}$  and  $^{241}\text{Pu}$  thermal cross sections were taken from ENDF/B-V<sup>29</sup> and the values listed Table IV were obtained by averaging over a 20° C Maxwellian spectrum. The actual values used in determining  $N_x/N_r$  were corrected for moderator temperature and a correction for epi-thermal neutrons was made according to a procedure described by Westcott.<sup>30</sup>

There is a problem connected with the  $^{239}\text{Pu}$  thermal fission cross section and the value used here follow an interim solution suggested by Poenitz.<sup>31</sup> Consistency fits to available data by Leonard and Thompson<sup>32</sup> and the preliminary results of an evaluation by Stehn et al.<sup>33</sup> have given 2200 m/sec cross sections of 754.8 b and 748.1 b, an increase of 1% or more compared to ENDF/B-V.<sup>29</sup> A similar analyses of the  $^{235}\text{U}$  data shows little change. Furthermore, comparisons of the masses of  $^{239}\text{Pu}$  and  $^{235}\text{U}$  samples at this laboratory using thermal neutrons differ from other methods by  $\sim 1.5\%$  when ENDF/B-V cross sections are used and suggest a larger value for  $^{239}\text{Pu}$ . For the present measurement, the shape of the  $^{239}\text{Pu}$  cross section given by ENDF/B-V was retained but the magnitude was scaled upward by 1.4% to give an average of the two evaluations at 2200 m/sec (752 b) with an estimated error of 0.5%.

## II.4 Corrections to the Data

### II.4.1. Backgrounds

There are two principal sources of background. The first is a general room return which consists of very low energy neutrons that show little time dependence over periods of a few  $\mu$ s. These neutrons produced ~ 1 to ~ 10% of the total fissions in the  $^{235}\text{U}$  detector, but had little effect on those isotopes with a definite fission threshold (e.g.  $^{238}\text{U}$ ). This background was measured by placing a time window over the time peak and a second window some 100 ns later. This procedure also served to correct for any alphas which exceeded the bias level and for any spontaneous fissions.

The second background source was produced by (d,n) reactions with the gas target structure, gas cell window and carbon deposits on the window and collimators. It generally increased with time, so it was measured with an empty gas cell both before and after each measurement with a full cell. For the  $^{235}\text{U}$  detector the correction ranged from ~ 2% at 2 MeV deuteron energy to ~ 20% at 7.5 MeV. The effect on the fission ratios was not nearly as large since most of these neutrons had energies high enough to cause fission in both samples.

At the highest proton energies some neutrons were produced by the Ta (p,n) reaction with the tantalum backing of the lithium target. This was not a serious background source; the neutron spectrum was similar to that produced by the  $^7\text{Li}(p,n^3\text{H})^4\text{He}$  reaction so it is included in that correction (See Section II.4.5.).

### II.4.2. Extrapolation to Zero Bias

The pulse height spectrum of those events falling within the time window was inspected and a cut-off point was selected in the flat region between the alphas and the fissions as illustrated in Fig. 2. The room-return background was subtracted and the spectrum was extended horizontally to the zero channel. This correction depended on the thickness and uniformity of the deposit but for most of the samples it fell within the 0.5 to 3% range.

### II.4.3. Scattered Neutrons

Although the timing requirements rejected fissions produced by neutrons scattered by distant objects they could not discriminate against those scattered by nearby objects such as the fission chamber and the neutron source structure. Corrections were calculated using the Monte Carlo code CYSCAT which is described in ref. 34. This program permits the inclusion of the source angular and energy distribution as well as energy dependent cross sections and angular distribution coefficients. It only considers single scattering but this should not be a serious fault; the correction was never more than a few percent and the double scattering contribution should be of the order of the square of that quantity. A more serious simplification lies in the handling of inelastic scattering which is the

principle contribution to the correction. All inelastic scattering was assumed to be isotropic and to have an energy distribution of the form

$$N(E) \propto E \exp(-E/\theta) \quad (9)$$

$$\theta \simeq 7.5 / \sqrt{A}$$

For  $^{235}\text{U}$ , fissions by scattered neutrons ranges from  $\sim 8\%$  near 0.3 MeV to  $\sim 2.5\%$  near 10 MeV. This effect was less for those isotopes with high fission thresholds since the energies of many of the inelastically scattered neutrons were too low in energy to cause fission. Thus for  $^{238}\text{U}$  the correction to the fission cross ratio is  $\sim 1.5\%$  but for  $^{233}\text{U}$  the correction is only  $\sim 0.1\%$ .

#### II.4.4. Deposit Thickness, Momentum Transfer and Fragment Angular Distribution

This correction is developed to first order in  $t/R$  in ref. 5. The fractional loss of fragments in the backward direction is

$$L_r \simeq -\omega(\pi/2) (t/2R + \gamma) \quad (10)$$

In the forward direction it is

$$L_f \simeq -\omega(\pi/2) (t/2R + R\gamma/2t - \gamma) \quad t > R\gamma \quad (11)$$

$$L_f = 0 \quad t > R\gamma \quad (12)$$

where  $R$  is the average fragment range,  $t$  is the deposit thickness,  $\omega(\pi/2)$  is the normalized fragment angular distribution evaluated at  $\pi/2$  and  $\gamma$  is the ratio of the velocity of the center mass to the velocity of the fragment in the center of mass system. When measurement are made with both fission chamber orientations and averaged, the correction to the average is

$$L_{av} = -\omega(\pi/2) (t/2R + R\gamma^2/4t) \quad t > R\gamma$$

$$L_{av} = -\omega(\pi/2) (t/4R + \gamma/2) \quad t < R\gamma$$

$R$  is strongly dependent on the actual composition of the fission deposit. It was determined for Th, U and Np by measuring the specific fission rates of a series of samples having a wide range of thicknesses. No such measurements were made for the plutonium samples. The composition of those samples was assumed to be  $\text{PuO}_2$ , and  $R$  was estimated from the range measurements of Alexander and Gazdik<sup>35</sup> and Niday<sup>36</sup>. The ranges used in the present measurements are:

U (SST and Mo series)	$4.7 \pm 1.0$	mg U/cm <sup>2</sup>
U (5 series)	$4.1 \pm 0.5$	mg U/cm <sup>2</sup>
Th	$5.1 \pm 0.3$	mg Th/cm <sup>2</sup>
Np	$5.6 \pm 1.4$	mg Np/cm <sup>2</sup>
Pu	(6.8)	mg Pu/cm <sup>2</sup>

### II.4.5. Isotopic Impurities and Neutron Spectrum

Neutrons were produced by charged particle reactions with lithium and deuterium targets. While the principal source reactions were  $^7\text{Li}(\text{p},\text{n})^7\text{Be}$  and  $\text{D}(\text{d},\text{n})^3\text{He}$ , neutrons with quite different energies could also be produced by the  $^7\text{Li}(\text{p},\text{n})^7\text{Be}^*$ ,  $^7\text{Li}(\text{p},\text{n}^3\text{H})^4\text{He}$  and  $\text{D}(\text{d},\text{pn})\text{D}$  reactions. Measurements of the neutron yields and energy distributions for these reactions, reported in refs. 37 and 38, were used to correct the ratio measurements.

It is convenient to represent the neutron spectrum by

$$M(E, \theta) = \sum_g A_g M_g(E, \theta)$$

where  $M_g(E, \theta)$  is the normalized energy and angle distribution function for source reaction  $g$  and  $A_g$  in the fraction of the total neutron yield produced by that reaction. The correction factor, in eq. (6), for the neutron spectrum and the minor isotopes can be expressed as

$$\frac{C_x}{C_r} = \frac{\sum_g A_g \int d\Omega \int M_g(E, \theta) \sum_i P_{xi} R_{2i}(E) dE}{\sum_g A_g \int d\Omega \int M_g(E, \theta) \sum_i P_{ri} R_{li}(E) dE} \quad (13)$$

$$R_{li} = \sigma_i(E)/\sigma_1(E_1) \quad (14)$$

$$R_{2i} = \sigma_i(E)/\sigma_2(E_1) \quad (15)$$

where  $E_1$  is the effective neutron energy of the principal neutron source reaction and the integration is carried out over the solid angle of the sample.

This correction requires some knowledge of the energy dependent fission cross sections for the isotopes involved and the Evaluated Nuclear Data File<sup>29</sup> provided this information. For fairly pure samples the minor isotopes are present in such small amounts that their cross sections need not be known very accurately. For the major isotopes an iterative procedure was used where the fission cross sections ratios obtained from one pass through the data were used as input for another pass.

### III. Errors

Table VI lists the sources of error in the normalization factor for the shape measurement and indicates the approximate contribution to the percentage error of each ratio measurement. The individual errors are described below and, where possible, their magnitudes are given.

(1) Half-lives. These are  $2\sigma$  values taken from the literature.<sup>24,25,28</sup>

(2) Thermal Fission Cross Sections. The important quantity is the ratio to  $^{235}\text{U}$ . Errors based on fits to the available data have generally been small although recent changes in the  $^{239}\text{Pu}$  values suggest larger uncertainties. For the present measurements the error in the thermal fission cross section ratios is assumed to be 0.5% and uncorrelated with any of the factors listed here. This is probably not completely true since alpha half-lives may be used to determine the sample weights in the thermal cross section measurements.

(3) Isotopic Analyses. For the present measurements the systematic error for those isotopes in the 1 - 10% range is 0.5%. There is 100% correlation for similar samples analyzed at the same time. Actually the error is larger for a single analyses at the level, but these analyses were usually the average of several measurements made over a period of months. The error is negligible for the major isotopes.

(4) Isotopic Dilution Analysis. A 0.5% systematic error is assumed for all such analyses. For all measurements using the same spiking solutions the correlation is 100%. Otherwise the correlation is zero. In practice this means no correlation between the several ratio measurements.

(5) Colorimetric Analysis. This is similar to (4) except the error is assumed to be 0.7%.

(6) Alpha Count (Systematic). This includes all the alpha counting errors except the statistical error. Most of the present measurements used the same low geometry counter so some sources of error were eliminated. Other sources of error were sample non-uniformity, small uncertainties in the distances to the aperture at the various shelf position, small variations in the sample radii and because some samples plates are not perfectly flat. An estimated error of 0.3% was assigned to each ratio measurement with no correlation between measurements.

There are two exceptions to the above value. In the  $^{238}\text{U}/^{235}\text{U}$  measurement the  $^{235}\text{U}$  samples were counted in the low geometry counter while the  $^{238}\text{U}$  samples were counted in a  $2\pi$  counter. The error was increased to 0.6%. For the  $^{242}\text{Pu}$  samples there was a problem in the spectrum analyses that caused the error to be set at 0.5%.

(7) Thickness Correction. The correction was calculated for each sample at the normalization energies and the uncertainty was set at 20% of the correction. For simplicity, it was assumed that this error was the same at all energies even though the correction does have a small energy dependence. The correlation with energy is 100% but between the various samples it is zero.

(8) Extrapolation. The systematic error to the ratio was placed at 0.2% and the correlation with energy at 100%.

(9) Dead Time Correction. This error applied only to the thermal calibration measurements at the ATSR. The systematic error to the fission cross section ratio is 0.5% for all measurements and the correlation is 100%.

(10) Scattering Correction. This error was assumed to be 30% of the calculated correction factor at 2.5 MeV neutron energy, but not less than 0.003. For simplicity it was assumed to be constant and 100% correlated with energy.

(11) Counting Statistics. This includes all counting statistic associated with the determination of the normalization factor; i.e. alpha-count, thermal calibration measurements, statistical error at the normalization points, etc.

There are additional errors that cannot be included in the normalization error but must be applied to the shape measurement:

(12) Neutron Spectrum. The error in the fission cross section ratio due to the secondary source reactions. These are set at 20% of the correction. All errors associated with a specific reaction are completely correlated but there is no correlation between the various reactions. This error is listed for each ratio in Table VII for representative energies.

(13) Neutron Energy. This is the apparent error in the fission cross section ratio caused by an error in the neutron energy. The error in the ratio, R, is given by

$$dR = \frac{dR}{dE} \Delta E \quad (16)$$

The energy error is primarily due to uncertainties in the thickness of the lithium targets and the gas cell windows and can be empirically related to the resolution. The error is largely systematic and a 100% correlation is assumed in the energy region of each target with no correlation between the targets. In the present measurement the energy error is estimated to be ~ 20% of the energy resolution and the cross section error can be obtained from the data in Tables VIII-XVII using eq. (16). The error can also be estimated from the other errors given in this report by

$$E_E = (E_t^2 - E_u^2 - E_n^2 - E_s^2)^{1/2} \quad (17)$$

where  $E_t$  is the total error in Tables VIII-XVII,  $E_u$  is the uncorrelated error in the same tables,  $E_n$  is the normalization error from Table VI and  $E_s$  is the neutron spectrum error from Table VII.

(14) Uncorrelated Error. This is listed in column 4 of Tables VIII-XVII. The principle component is the counting statistics, but a part is based on the consistency of repeated measurements. Under normal operating conditions the scatter is larger than can be accounted for by counting statistics alone by an amount equivalent to  $\sim 0.5\%$  per measurement. This was combined with the counting statistics to give the uncorrelated error. For the  $^{240}\text{Pu}$  ratio the scatter was  $\sim 1.5\%$ .

#### IV. Results and Discussion

Tables VIII-XVII list the results of these ratio measurements and also include the fission cross section values obtained using the  $^{235}\text{U}$  fission cross section file from ENDF/B-V<sup>29</sup>. In Figs. 3-12 they are compared with fission cross section ratios and fission cross sections from ENDF/B-V.

The results depend to a degree on secondary data such as alpha half-lives and thermal fission cross sections and Table XVIII shows the effect of changes in these quantities on the cross section ratios. The relation is

$$\frac{dR}{R} = k \frac{dQ}{Q} \quad (18)$$

where  $R$  is the cross section ratio,  $Q$  is the quantity changed and  $k$  is the factor given in Table XVIII. The effect of any changes in the weights of the "standard" samples (see Section II.3.) are also listed. However, these are redundant if they are due to changes in the secondary data.

Three of the "standard" samples (5-1, 5-2 and SST-5) were among those used in a comparison of reference  $^{235}\text{U}$  samples from several laboratories.<sup>21</sup> The sample weights listed in Table I of this report are comparable with the "quoted masses" in Table 9 of ref. 21. They are not in exact agreement because they are based on a different value of the  $^{234}\text{U}$  half-life and a different set of alpha counts. Samples 5-1 and 5-2 are in good agreement with the results of the comparison but SST-5 is low by  $\sim 1.5\%$ . Table XVIII shows that only the  $^{237}\text{Np}/^{235}\text{U}$  result will be significantly affected by such a change and it will be increased by 0.75%. Ratios other than those indicated in Table XIX use SST samples but those are cases where  $N_x/N_r$  is measured and the actual masses do not appear.

The present results are based on a number of additional measurements that were not available for the original reports. The  $^{233}\text{U}/^{235}\text{U}$  ratio measurements were made before the methods for calculating corrections for the  $^7\text{Li}(p, n^3\text{He})^4\text{He}$  and  $D(d, np)D$  reactions were available, so no data

were reported in the 3 - 4.7 and 7.3 - 10 MeV regions. Additional measurements were made for this report in order to better define the shape and confirm the normalization. All the older data were reprocessed, beginning with the original fission rate measurements. The  $^{238}\text{U}/^{235}\text{U}$  ratio measurements, reported in ref. 1, used time-of-flight over a 52 cm path to eliminate the fissions produced by neutrons from the  $^7\text{Li}(\text{p},\text{n}^3\text{H})^4\text{He}$  reaction. Since that time, additional measurements have been made in that region and corrections calculated using the method of section II.4.5, and they are included in this report. All the  $^{238}\text{U}$  data were reprocessed. The normalization of the  $^{242}\text{Pu}/^{235}\text{U}$  measurements, reported in ref. 7, was based solely on alpha counting. The present results include additional normalization data based on relative thermal fission rates.

There are a number of small changes in the revised data. The average energies and energy resolutions of all points were recalculated as described in Section II.2.5. This increased the energies of the older measurements by  $\sim 2$  keV near 0.2 MeV neutron energy,  $\sim 10$  keV near 4 MeV and  $\sim 50$  keV near 10 MeV. There was little change in the shape measurements but there were some noticeable changes in normalization. These are listed in Table XIX; they average  $\sim 0.7\%$  with a maximum of 1.85%. The revised half-lives and thermal fission cross sections are important contributors to these normalization differences, particularly for  $^{239}\text{Pu}/^{235}\text{U}$  where they account for about half of the 1.85% change. Other differences come from revisions in the procedures for calculating the several correction factors, the inclusion of additional normalization measurements and the different positions of the time windows and bias levels used in reprocessing the data. No single one of these produces a really significant effect but if several of them are in the same direction they can easily produce the observed changes.

## V. Summary

The results of previous measurements at this laboratory of the fission cross sections of some thorium, uranium, neptunium and plutonium isotopes relative to  $^{235}\text{U}$  have been reviewed and revised to include changes in data processing procedures, alpha half-lives and thermal fission cross sections. Some new data have been included and the question of errors has been re-examined and put on a more consistent basis. The energies of the older measurements have been increased by amounts ranging from 1 - 2 keV near 0.2 MeV neutron energy to 50 keV near 10 MeV. There has been little change in the shape measurements but the normalizations have changed by amounts ranging from  $-1.77\%$  ( $^{233}\text{U}/^{235}\text{U}$ ) to  $+1.85\%$  ( $^{239}\text{Pu}/^{235}\text{U}$ ).

## VI. References

1. J. W. Meadows, Nucl. Sci. Eng., 49, 310 (1972).
2. J. W. Meadows, Nucl. Sci. Eng., 54, 312 (1974).
3. J. W. Meadows, Nucl. Sci. Eng. 58, 255 (1975).
4. J. W. Meadows, "The Fission Cross Sections of Uranium and Plutonium Isotopes Relative to U-235", Proc. NEANDC/NEACRP Specialists Meeting on Fast Neutron Fission Cross Sections of U-233, U-238 and Pu-239, June 28-30, 1976, ANL-76-90, p. 73, Argonne National Laboratory (1976).
5. J. W. Meadows, "The Fission Cross Section of  $^{239}\text{Pu}$  Relative to  $^{235}\text{U}$  from 0.1 to 10 MeV", ANL/NDM-39, Argonne National Laboratory (1978).
6. J. W. Meadows, Nucl. Sci. Eng. 65, 171 (1978).
7. J. W. Meadows, Nucl. Sci. Eng. 68, 360 (1978).
8. J. W. Meadows, "The Fission Cross Section of  $^{230}\text{Th}$  and  $^{232}\text{Th}$  Relative to  $^{235}\text{U}$ ", Proc. Intl. Conf. Nuclear Cross Sections for Technology, Knoxville, Tennessee, October 22-26, 1979, NBS Special Publication 594, p. 479, U. S. National Bureau of Standards (1980).
9. J. W. Meadows, Nucl. Sci. Eng., 79, 233 (1981).
10. J. W. Meadows, submitted to Nuclear Sci. Eng.
11. J. W. Meadows, D. L. Smith and G. Winkler, Nucl. Instr. and Methods, 176, 439 (1980).
12. C. Budtz-Jørgensen and H.H. Knitter, Nucl. Sci. Eng. 79, 380 (1981).
13. C. Bonnet, P. Hillion and C. Nardin, Nucl. Inst. and Methods, 54, 32 (1967).
14. Benjamin P. Burtt, Nucleonics 5, p. 28, (Aug., 1949).
15. J. W. Meadows, "Determination of the Energy Scale for Neutron Cross Section Measurements Employing a Monoenergetic Accelerator", ANL/NDM-25, Argonne National Laboratory (1977).

16. J. B. Marion, *Rev. Mod. Phys.* 38, 660 (1966).
17. E. H. Beckner, R. L. Bramblett, G. C. Phillips and T. A. Eastwood, *Phys. Rev.*, 123, 2100 (1961).
18. H. H. Anderson and J. F. Fugler, "Hydrogen Stopping Powers and Ranges in all Elements", Vol. 3 of "The Stopping and Ranges of Ions in Matter", Pergamon Press, New York (1977).
19. Horst Liskien and Arno Paulsen, *Atomic Data and Nuclear Data Tables*, 15, 57 (1975).
20. Horst Liskien and Arno Paulsen, *Nuclear Data Tables*, 11, 569 (1973).
21. W. P. Poenitz, J. W. Meadows and R. J. Armani, "<sup>235</sup>U Fission Mass Standardization and Intercomparison", ANL/NDM-48, Argonne National Laboratory (1979).
22. W. Parker, H. Bildstein and N. Getoff, *Nucl. Instr. Methods*, 26, 55 (1964).
23. R. Ko, "Electrodeposition of the Actinide Elements", HW-41025, Hanford Atomic Products Report (1956).
24. N. E. Holden, "The Uranium Half-lives: A Critical Review", BNL-NCS-51320, Information Analysis Center Report, National Nuclear Data Center, Brookhaven National Laboratory (1981).
25. "Proposed Recommended List of Transactinium Isotope Decay Data. Part I. Half-Lives", A. Lorenz, editor, INDC(NDS)-108/N, IAEA Nuclear Data Section, Vienna (1979).
26. J. W. Meadows, "The Alpha and Spontaneous Fission Half-Lives of <sup>242</sup>Pu", ANL/NDM-38, Argonne National Laboratory (1977).
27. J. W. Meadows, R. J. Armani, E. L. Callis and A. M. Essling, *Phys. Rev. C* 22, 750 (1980).
28. F. P. Brauer, R. W. Stromatt, J. D. Ludwick, F. P. Roberts and W. L. Lyons, *J. Inorg. Nucl. Chem.*, 12, 234 (1960).
29. Evaluated Nuclear Data File, ENDF/B-V; See also ENDF/B Summary Documentation, BNL-NCS-17541 (ENDF-201), 3rd. ed., R. Kinsey, ed., National Nuclear Data Center, Brookhaven National Laboratory (1979).

30. C. H. Westcott, "Effective Cross Section Values for Well Moderated Thermal Reactor Spectra", CRRP-787, Atomic Energy of Canada Limited, Chalk River Project (1958).
31. W. P. Poentiz, Private Communication (1982).
32. B. R. Leonard, Jr. and J. K. Thompson, "Evaluation of the Thermal Cross Sections of  $^{239}\text{Pu}$  and  $^{241}\text{Pu}$ ", EPRI-NP-1763, Electric Power Research Institute (1981).
33. J. R. Stehn, M. Divadeenam and N. E. Holden, "Evaluation of the Thermaen Neutron Constants for  $^{233}\text{U}$ ,  $^{235}\text{U}$ ,  $^{239}\text{Pu}$  and  $^{241}\text{Pu}$ ", Proc. Intl. Conf. Nuclear Data for Science and Technology, Antwerp, 6-10 September 1982, D. Reidel Publishing Company, Dordresht, Holland (1982).
34. D. L. Smith and J. W. Meadows, "Neutron Inelastic Scattering Studies for Lead-204", ANL/NDM-37, Argonne National Laboratory (1977).
35. J. M. Alexander and M. F. Gazdik, Phys. Rev., 120, 874 (1960).
36. J. B. Niday, Phys. Rev., 121, 1471 (1961).
37. J. W. Meadows and D. L. Smith, "Neutrons from Proton Bombardment of Natural Lithium", ANL-7938, Argonne National Labortory (1972).
38. D. L. Smith and J. W. Meadows, "A Method of Neutron Activation Cross Section Measurement Using the  $\text{D}(\text{d},\text{n})^3\text{He}$  Reaction as a Neutron Source", ANL/NDM-9, Argonne National Laboratory (1974).
35. J. M. Alexander and M. F. Gazdik, Phys. Rev., 120, 874 (1960).
36. J. B. Niday, Phys. Rev., 121, 1471 (1961).
37. J. W. Meadows and D. L. Smith, "Neutrons from Proton Bombardment of Natural Lithium", ANL-7938, Argonne National Labortory (1972).
38. D. L. Smith and J. W. Meadows, "A Method of Neutron Activation Cross Section Measurement Using the  $\text{D}(\text{d},\text{n})^3\text{He}$  Reaction as a Neutron Source", ANL/NDM-9, Argonne National Laboratory (1974).
35. J. M. Alexander and M. F. Gazdik, Phys. Rev., 120, 874 (1960).
36. J. B. Niday, Phys. Rev., 121, 1471 (1961).

37. J. W. Meadows and D. L. Smith, "Neutrons from Proton Bombardment of Natural Lithium", ANL-7938, Argonne National Labortory (1972).
38. D. L. Smith and J. W. Meadows, "A Method of Neutron Activation Cross Section Measurement Using the D(d,n)<sup>3</sup>He Reaction as a Neutron Source", ANL/NDM-9, Argonne National Laboratory (1974).

Table I. The Isotopic Analyses and Masses of the Uranium Samples.

Sample No.	Isotopic Analyses (Mole %)						Wt. Element ( $\mu$ g)	Assay <sup>a</sup> Method	
	232	233	234	235	236	238			
<u>U-233</u>									
233 - 1002	0.8 ppm						216.7	3	
233 - 1202		99.540	0.184	0.062	0.013	0.203	253.4	3	
233 - 1402							296.3	3	
<u>U-234</u>									
234 - 5	--	--	99.900	0.064	0.036	< 0.070	420.0	3	
234 - 31	--	--					187.9	3	
234 - 32		--	89.95	9.92	0.053	0.075	361.5	3	
234 - 33							591.4	3	
<u>U-235</u>									
235 - 1	--						762.2	8	
235 - 2		--	0.028	99.856	0.062	0.054	598.8	8	
235 - 3							390.3	8	
235 - 7	--	1.537	0.046	98.011	0.318	0.088	359.0	3	
235 - 5	--	3.064	0.049	96.467	0.314	0.106	332.6	3	
235 - 6	--						285.7	3	
235 - 10		--	5.127	0.050	94.220	0.307	0.094	266.5	3
235 - 12							290.7	3	
235 - 14							358.8	3	
235-SST-1							658.7	3,4,2	
235-SST-5	--	--	0.856	93.244	0.332	5.568	412.8	3,4,2	
235-SST-6		--					1855	3,4,2	
235-SST-8							1008	3,4,2	
235 5-1	--	--	1.032	98.409	0.455	0.102	1066	3,4,2,1	
235 5-2							833.8	3,4,2,1	

Table I. The Isotopic Analyses and Masses of the Uranium Samples. (Continued)

Sample No.	Isotopic Analyses (Mole %)						Wt. Element (μg)	Assay <sup>a</sup> Method
	232	233	234	235	236	238		
<u>U-238</u>								
238 SST-26							1004	4,2
238 Mo-4	—	—	0.003	0.415	—	99.585	1782	4,2
238 Mo-8							5330	4,2
238 8-1							733.8	8
238 8-2	—	—	0.114	10.084	0.050	88.993	599.8	8
238 8-3							370.3	8
238 - 60	←	—	< 0.6 ppm	—	→ 100.00		1981	8
236 - 6	—	—		0.402	99.593	0.011	666.6	3
236 - 35	—	—	0.015	13.640	86.190	0.160	295.0	3
236 - 36	—	—	0.004	11.000	88.840	0.160	618.1	3

<sup>a</sup>Assay methods are defined in Section II.3.2.

Table II. Isotopic Analyses and Masses of the Thorium and Neptunium Samples

Sample No.	Isotopic Analyses (Mole %)				Wt. Element ( $\mu$ g)	Assay <sup>a</sup> Method
	230	232	237	239		
Th-230						
230 - 51					405.5	1
230 - 53	99.516	0.484			483.7	4
230 - 54					774.2	4
230 - 55					380.8	1
Th-232						
232 - 3	0.379	99.621	100.0			8
232 - 32					706.6	1
232 - 33					1971.0	1
232 - 34					2903.8	4
232 - 35					674.8	1
232 - 36					1279.5	1
Np-237						
237 - 79			100.0		660.4	3

<sup>a</sup>Assay methods are defined in Section II.3.2.

Table III. The Isotopic Compositions and Masses of the Plutonium Samples.

Sample No.	Isotopic Analyses (Mole %)						Wt. μg	Assay <sup>a</sup> Method
	238	239	240	241	242	Am-241		
<u>Pu-239</u>								
239 - 267	--	99.952	0.048	--	--	--	130.0	3
<u>Pu-240</u>								
240 - 38	0.012	0.677	98.386	0.426	0.370	0.128	75.4	3
240 - 39	0.012	0.674	98.394	0.421	0.370	0.129	259.6	3
240 - 40	0.009	9.490	89.634	0.381	0.338	0.148	94.4	3,1
240 - 41	0.016	9.330	89.825	0.384	0.336	0.110	335.4	3,1
<u>Pu-242</u>								
242 - 42	--	0.008	0.106	0.136	99.744	--	383.3	3
242 - 44							374.3	3
242 - 49	0.007	9.128	0.097	0.099	90.169	--	219.2	3

<sup>a</sup>Assay methods are defined in Section II.3.2.

Table IV. The Half-Lives and Thermal Fission Cross Sections Used in the Measurements

Isotope	Half-Life (years)		$\sigma_F$ (barns) (200°C Maxwellian)
	Alpha	Spontaneous Fission	
$^{230}\text{Th}$	$7.538 \times 10^4$ <sup>a</sup>	---	---
$^{232}\text{Th}$	$1.405 \times 10^{10}$ <sup>d</sup>	---	---
$^{233}\text{U}$	$1.592 \times 10^5$ <sup>c*</sup>	---	526.6 <sup>f,*</sup>
$^{234}\text{U}$	$2.455 \times 10^5$ <sup>c*</sup>	---	---
$^{235}\text{U}$	$7.037 \times 10^8$ <sup>c</sup>	---	570.4 <sup>f,*</sup>
$^{236}\text{U}$	$2.342 \times 10^7$ <sup>c*</sup>	---	---
$^{238}\text{U}$	$4.468 \times 10^9$ <sup>c</sup>	---	---
$^{237}\text{Np}$	$2.14 \times 10^6$ <sup>e*</sup>	---	---
$^{239}\text{Pu}$	24110 <sup>d*</sup>	---	792.6 <sup>g,*</sup>
$^{240}\text{Pu}$	6569 <sup>d*</sup>	$1.31 \times 10^{11}$ <sup>d</sup>	1060.9 <sup>f</sup>
$^{241}\text{Pu}$	14.7 <sup>d</sup>	---	---
$^{242}\text{Pu}$	$3.736 \times 10^5$ <sup>b</sup>	$6.79 \times 10^{10}$ <sup>b</sup>	---
$^{241}\text{Am}$	432.6 <sup>d</sup>	---	---

\*These values are of particular importance for determining the weights of some of the samples.

<sup>a</sup>Ref. 27.

<sup>b</sup>Ref. 26.

<sup>c</sup>Ref. 24.

<sup>d</sup>Ref. 25.

<sup>e</sup>Ref. 28.

<sup>f</sup>Ref. 29.

<sup>g</sup>See Section II.3.2.

Table V. The Average Fission Cross Section Ratios at the Normalization Energies  
Classified According to the Assay Method (Continued)

Sample Nos.	α Count			Thermal Fission			Isotopic Dilution
	Common α Emitter	Calc. Sp. Activity	Meas. Sp. Activity	Common Isotope	Relative Thermal α		
Th-230/U-235							
230-51/235 5-2	--	--	--	--	--	--	0.2328
230-53/235 5-2	--	--	0.2313	--	--	--	--
230-54/235 5-2	--	--	0.2327	--	--	--	--
230-55/235 5-2	--	--	--	--	--	--	0.2304
Th-232/U-235							
232-32/235 5-2	--	--	--	--	--	--	0.1036
232-33/235 5-2	--	--	--	--	--	--	0.1023
232-34/235 5-2	--	--	0.1022	--	--	--	--
232-35/235 5-2	--	--	--	--	--	--	0.1026
232-36/235 5-2	--	--	--	--	--	--	0.1029
U-233/U-235							
233-1002/235-6	1.514	--	--	--	1.562	--	--
233-1002/235-10	1.531	--	--	--	1.548	--	--
233-1202/235-12	1.551	--	--	--	1.560	--	--
233-1202/235-5	1.538	--	--	--	1.542	--	--
233-1202/235-5-2	--	1.520	--	--	1.527	--	--
233-1402/235-14	1.523	--	--	--	1.553	--	--
233-1402/235-7	1.574	--	--	--	1.534	--	--
233-1402/235-3	--	1.515*	--	--	1.508	--	--

Table V. The Average Fission Cross Section Ratios at the Normalization Energies  
Classified According to the Assay Method (Continued)

Sample Nos.	α Count		Thermal Fission			
	Common α Emitter	Calc. Sp. Activity	Meas. Sp. Activity	Common Isotope	Relative Thermal $\sigma$	Isotopic Dilution
U-234/U-235						
234-5/235 5-2	1.191	--	--	--	--	--
234-31/235 SST-5	1.230	--	--	1.234	--	--
234-32/235 5-1	1.189	--	--	1.191	--	--
234-33/235-14	--	1.201	--	1.203	--	--
U-236/U-235						
236-6/235-2	--	0.6936	--	--	--	--
236-35/235-14	--	0.6845	--	0.6921	--	--
236-36/235-1	--	--	--	0.6967	--	--
U-238/U-235						
238 8-1/235-1	--	--	--	0.4351	--	--
238 8-2/235-2	--	--	--	0.4333	--	--
238 8-3/235-3	--	--	--	0.4392	--	--
238 M0-8/236 SST-8	--	--	0.4288	--	--	--
238 M0-4/235 SST-6	--	--	0.4345	--	--	--
Np-237/U-235						
237-79/235 SST-1	--	1.326	--	--	--	--
237-79/235 SST-5	--	1.315	--	--	--	--

Table V. The Average Fission Cross Section Ratios at the Normalization Energies  
Classified According to the Assay Method

Sample Nos.	α Count			Thermal Fission		
	Common α Emitter	Calc. Sp. Activity	Meas. Sp. Activity	Common Isotope	Relative Thermal $\sigma$	Isotopic Dilution
237-79/235 5-2	--	1.329	--	--	--	--
237-79/235-14	--	1.327	--	--	--	--
Pu-239/U-235						
239-267/235 5-2	--	1.542	--	--	1.532	--
Pu-240/U-235						
240-38/235 5-1	--	1.336	--	--	--	1.342
240-38/235 5-2	--	1.342	--	--	--	1.350
240-39/235 5-2	--	1.350	--	--	--	--
240-40/235 5-2	--	1.332	--	--	1.332	1.341
240-41/235 5-1	--	1.339	--	--	1.338	1.317
Pu-242/U-235						
242-42/235-3	--	1.113*	--	--	--	--
242-49/235-14	--	1.145	--	--	1.110	--
242-44/235-3	--	1.117*	--	--	1.097	--
242-49/235 SST-5	--	1.108	--	--	1.116	--
242-44/235 5-2	--	1.124	--	--	1.079	--

\* The mass of uranium sample 235-3 was determined by comparing its fission rate with the fission rate of other 235 samples. Since the masses of most of these samples were based on this calculated specific activity the 235-3 measurements are listed in that column.

Table VI. The Various Sources of Error Contributing to the Total Error in Normalization

Source of Error	% Error in the Ratio									
	230Th	232Th	233U	234U	236U	238U	237Np	239Pu	240Pu	248Pu
half-lives U 233	--	--	--	0.03	0.03	--	0.04	--	--	0.02
U 234	0.12	0.12	0.02	--	0.06	--	0.08	0.12	0.08	0.05
U 236	--	--	--	--	0.08	--	--	--	--	--
Np 237	--	--	--	--	--	--	0.45	--	--	--
Pu 239	--	--	--	--	--	--	--	0.05	--	0.05
Pu-240	--	--	--	--	--	--	--	--	0.03	--
$\alpha$ th	233/235	--	--	0.25	--	--	--	--	--	--
	239/235	--	--	--	--	--	--	0.25	0.17	0.25
Isotopic Analysis	0.25	0.25	0.25	0.29	0.31		0.31	0.19	0.14	0.32
Isotopic Dilution	0.56	0.56	--	--	--	--	0.08	--	0.24	0.25
Colorimetric	0.16	0.16	--	--	--	0.50	0.08	--	0.16	0.10
$\alpha$ -counts Syst.	0.30	0.38	0.15	0.15	0.15	0.60	0.30	0.15	0.20	0.52
Thickness Corr.	0.41	0.30	0.10	0.10	0.18	0.18	0.40	0.19	0.22	0.10
Extrapolation	0.20	0.20	0.10	0.10	0.10	0.10	0.20	0.20	0.40	0.20
Dead Time Corr.	--	--	0.25	0.25	0.25	0.25	--	0.25	--	0.25
Scattering Corr.	0.60	0.60	0.30	0.60	0.45	0.60	0.30	0.30	0.30	0.30
Statistical	0.59	0.57	0.50	0.35	0.55	0.42	0.30	0.55	0.82	0.60
Total Error	1.19	1.17	0.82	0.82	0.86	1.12	0.89	0.82	1.07	1.04

Table VII. The Error in the Fission Cross Section Ratios Due to the Secondary Source Reactions

Neutron Energy (MeV)	% Error in the Ratio									
	230Th	232Th	233U	234U	236U	238U	237Np	239Pu	240Pu	242Pu
0.7 <sup>a</sup>	-	-	0	0	0	-	0	0	0.08	-
0.8	0.15	-	0	0.20	0.21	-	0.23	0.09	0.22	0.18
0.9	0.20	-	0.02	0.30	0.37	0.38	0.33	0.04	0.34	0.30
1.0	0.24	-	0.05	0.26	0.49	0.50	0.32	0.02	0.32	0.39
1.1	0.28	-	0.05	0.20	0.62	0.58	0.24	0.02	0.27	0.40
1.2	0.31	0.40	0.04	0.06	0.62	0.57	0.16	0.01	0.19	0.22
1.3	0.34	0.37	0.04	0.10	0.56	0.72	0.10	0.02	0.11	0.19
1.4	0.37	0.43	0.03	0.05	0.50	0.84	0.06	0.17	0.03	0.14
1.5	0.21	0.50	0.02	0.12	0.42	0.94	0.05	0.13	0.04	0.12
1.7	0.07	0.49	0	0.15	0.13	0.90	0.02	0.09	0.01	0.11
1.8	0.06	0.20	0	0.14	0.14	0.80	0.02	0.04	0.03	0.06
2.0	0.04	0.19	0.01	0.05	0.20	0.34	0.02	0.01	0.01	0.01
3.0 <sup>b</sup>	0.06	0.05	0.01	0	0.06	0	0.02	0.02	0.12	0.04
3.5	0.32	0.40	0.01	0.20	0.30	0.42	0	0.05	0.30	0.18
4.0	0.72	1.32	0.04	0.40	0.68	1.17	0.10	0.08	0.48	0.34
4.5	1.54	2.62	0.07	1.06	1.49	2.15	0.03	0.20	0.92	0.76
5.0	2.42	-	-	2.24	-	4.45	-	0.31	-	-
6.0 <sup>c</sup>	0	0	0	0	0	0	0	0	0	0
8.0	0		0	0	0	0	0	0	0	0
8.5	0.26	.50	0.10	0.07	0.20	0.21	0.02	0.12	0.01	0.01
9.0	0.58	.87	0.22	0.09	0.40	0.75	0.03	0.30	0.10	0.04
9.5	0.95	.92	0.30	0.11	0.69	1.20	0.06	0.42	0.10	0.04
10.0	-	1.20	-	0.07	1.17	1.36	-	0.86	-	0.13

<sup>a</sup>For neutron energies below 3 MeV the secondary reaction is  $^7\text{Li}(\text{p},\text{n})^7\text{Bi}^*$ .

<sup>b</sup>For neutron energies between 3 and 5 MeV the  $^7\text{Li}(\text{p},^3\text{H})^4\text{He}$  reaction is the principal error source.

<sup>c</sup>For the gas target the error source is the  $\text{D}(\text{d},\text{np})\text{D}$  reaction.

TABLE VIII. THE TH-230/U-235 FISSION CROSS SECTION RATIOS  
AND THE RESULTANT TH-230 FISSION CROSS SECTIONS.

ENERGY (MEV)	ENERGY RESOLUTION <sup>a</sup> (MEV)	CROSS SECTION RATIO	UNCORR. ERROR (%)	TOTAL ERROR (%)	CROSS SECTION <sup>b</sup> (B)
.737	.052	.0337	2.65	4.93	.384
.767	.052	.02842	3.02	7.17	.3231
.799	.052	.01056	4.83	7.34	.1203
.830	.052	.01051	5.22	5.34	.1201
.860	.052	.01430	4.76	10.98	.1646
.892	.052	.02751	3.56	11.42	.3204
.923	.052	.0411	2.48	11.06	.487
.956	.050	.0563	2.24	9.50	.678
.987	.048	.0693	2.01	9.11	.844
1.017	.048	.0998	1.74	10.33	1.216
1.048	.048	.1377	1.56	6.84	1.673
1.078	.048	.1669	1.54	4.41	2.028
1.105	.044	.1628	1.28	4.32	1.978
1.107	.048	.1757	1.49	3.23	2.136
1.140	.044	.1881	1.24	2.52	2.287
1.170	.044	.2055	1.21	2.54	2.502
1.200	.042	.2172	1.22	2.55	2.650
1.232	.042	.2359	1.18	2.09	2.883
1.261	.040	.2387	1.16	1.65	2.922
1.292	.040	.2287	1.15	2.15	2.807
1.323	.040	.2132	1.24	2.54	2.624
1.357	.040	.1986	1.22	1.69	2.451
1.383	.040	.2183	1.22	3.08	2.701
1.402	.068	.2175	1.06	2.55	2.695
1.413	.040	.2301	1.19	1.67	2.855
1.452	.066	.2170	1.03	2.68	2.703
1.502	.064	.1988	1.06	2.33	2.488
1.551	.064	.1917	1.11	1.63	2.411
1.500	.064	.2046	1.06	2.10	2.586
1.650	.064	.2143	1.04	2.35	2.724
1.701	.064	.2374	.99	2.14	3.035
1.750	.062	.2441	.97	1.70	3.132
1.800	.060	.2509	1.02	1.51	3.232
1.850	.060	.2433	.91	1.53	3.141
1.899	.060	.2358	.90	1.65	3.051
2.003*	.118	.2250	.52	1.24	2.921
2.124	.112	.2256	.96	1.47	2.923
2.250	.108	.2367	.94	1.45	3.051
2.374	.108	.2251	.11	1.53	2.882
2.498*	.104	.2355	.41	1.18	2.988

TABLE VIII. T (CONTINUED)

ENERGY (MEV)	ENERGY RESOLUTION <sup>a</sup> (MEV)	CROSS SECTION RATIO	UNCORR. ERROR (%)	TOTAL ERROR (%)	CROSS SECTION <sup>b</sup> (R)
2.747*	.100	.2345	.38	1.17	.2920
2.993*	.094	.2328	.34	1.16	.2840
3.241	.090	.2331	.86	1.41	.2792
3.489	.088	.2403	.91	1.47	.2825
3.984	.080	.2520	1.08	1.71	.2855
4.233	.076	.2481	1.00	1.82	.2790
4.481	.076	.2472	.10	2.15	.2750
4.664	.310	.2386	1.38	1.77	.2614
4.730	.076	.2449	1.10	2.46	.2668
4.977	.072	.2414	1.12	2.89	.2574
4.980	.248	.2337	1.75	2.07	.2491
5.308	.223	.2355	1.11	1.57	.2468
5.577	.207	.2318	1.34	1.74	.2431
5.838	.192	.2290	1.29	1.70	.2456
6.130	.180	.2445	1.14	2.17	.2870
6.398	.167	.2792	1.06	2.28	.3644
6.659	.154	.314	1.21	2.38	.452
6.887	.146	.366	1.12	2.25	.555
7.147	.138	.410	1.04	1.76	.660
7.403	.133	.429	1.01	1.50	.726
7.677	.128	.420	.99	1.50	.736
7.926	.126	.411	1.01	1.52	.730
8.172	.124	.393	1.01	1.52	.702
8.417	.122	.380	1.00	1.57	.677
8.646	.120	.370	1.39	.18	.659
8.890	.120	.369	1.03	1.61	.655
9.133	.120	.362	1.01	1.64	.640
9.378	.121	.353	.87	1.69	.622

\*Normalization points.

<sup>a</sup>Full-width-at-half-maximum.

<sup>b</sup>Based on the <sup>235</sup>U fission cross section from ENDF/B-V (ref. 29).

TABLE IX: THE TH-232/U-235 FISSION CROSS SECTION RATIOS  
AND THE RESULTANT TH-232 FISSION CROSS SECTIONS.

ENERGY (MEV)	ENERGY RESOLUTION <sup>a</sup> (MEV)	CROSS SECTION RATIO	UNCORR. ERROR (%)	TOTAL ERROR (%)	CROSS SECTION <sup>b</sup> (B)
1.267	.038	.00953	2.02	5.32	.01167
1.292	.037	.01130	1.86	10.83	.01387
1.316	.037	.01762	1.54	10.84	.02167
1.341	.037	.02310	1.44	7.57	.02848
1.367	.037	.02927	1.32	7.16	.03617
1.391	.036	.0367	1.24	8.14	.0454
1.417	.037	.0486	1.16	4.50	.0604
1.429	.036	.0449	1.42	1.92	.0558
1.466	.036	.0504	1.15	2.14	.0628
1.490	.035	.0520	1.34	3.20	.0650
1.514	.036	.0593	1.12	4.39	.0743
1.540	.032	.0691	1.30	4.12	.0868
1.565	.035	.0791	1.06	5.62	.0997
1.590	.034	.0945	1.21	1.76	.1193
1.605	.034	.0840	1.06	2.61	.1062
1.639	.034	.0830	1.22	1.92	.1054
1.691	.031	.0790	1.39	2.06	.1008
1.716	.031	.0801	1.39	2.12	.1024
1.741	.031	.0628	1.42	2.70	.0805
1.791	.031	.0628	1.42	2.70	.0808
1.841	.031	.0775	1.38	2.94	.1001
1.889	.030	.0931	1.35	2.08	.1204
1.939	.031	.0967	1.35	1.80	.1253
1.963	.080	.0951	.87	1.48	.1233
1.997*	.115	.0956	.30	1.59	.1240
2.024	.116	.1025	1.28	2.32	.1330
2.122	.112	.1052	.88	3.45	.1363
2.176	.112	.1155	1.26	1.16	.1493
2.277	.108	.0967	1.35	2.79	.1245
2.371	.108	.0968	.99	1.54	.1239
2.382	.106	.0933	1.08	1.60	.1193
2.449	.076	.0994	.74	1.39	.1266
2.494*	.105	.0959	.74	1.41	.1216
2.485	.104	.0974	1.08	1.62	.1237
2.687	.100	.1038	1.09	1.87	.1299
2.746	.100	.1072	1.00	1.83	.1335
2.788	.096	.1080	.99	1.82	.1340
2.889	.096	.1134	.96	1.76	.1395
2.953	.072	.1145	.70	1.50	.1401
2.954	.094	.1144	.93	1.68	.1400

TABLE IX. THE (CONTINUED)

ENERGY (MEV)	ENERGY RESOLUTION <sup>a</sup> (MEV)	CROSS SECTION RATIO	UNCORR. ERROR (%)	TOTAL ERROR (%)	CROSS SECTION <sup>b</sup> (R)
2.987*	.095	.1169	.61	1.52	.1426
3.232	.090	.1214	.77	1.44	.1455
3.243	.089	.1211	.77	1.46	.1450
3.478	.088	.1246	1.01	1.62	.1466
3.492	.085	.1239	1.01	1.62	.1456
3.724	.081	.1284	.99	1.70	.1482
3.743	.086	.1300	.95	1.68	.1499
3.972	.078	.1314	1.24	2.16	.1490
4.238	.078	.1337	.93	2.43	.1503
4.486	.075	.1380	1.04	3.07	.1534
4.736	.073	.1400	1.00	4.03	.1524
5.106	.223	.1370	1.14	1.64	.1448
5.596	.206	.1391	1.06	1.59	.1459
5.870	.192	.1382	1.22	1.70	.1490
6.142	.180	.1497	1.10	1.65	.1766
6.409	.166	.2038	1.00	1.58	.2672
6.673	.154	.2447	.94	1.51	.3532
6.931	.145	.2598	.92	1.50	.3977
7.188	.138	.2580	.94	1.51	.4195
7.444	.132	.2469	.94	1.51	.4205
7.693	.128	.2319	.94	1.51	.4065
7.944	.125	.2193	.96	1.52	.3909
8.194	.124	.2100	.96	1.52	.3747
8.443	.122	.2098	1.04	1.65	.3740
8.687	.120	.1971	1.01	1.58	.3505
8.934	.120	.1965	1.00	1.71	.3484
9.177	.120	.1987	1.01	1.84	.3513
9.419	.120	.1959	1.04	2.05	.3455
9.663	.121	.1914	1.07	2.30	.3364
9.904	.122	.1885	1.30	2.50	.3302

\*Normalization points.

<sup>a</sup>Full-width-at-half-maximum.

<sup>b</sup>Based on the  $^{235}\text{U}$  fission cross section from ENDF/B-V (ref. 29).

TABLE X. THE U-233/U-235 FISSION CROSS SECTION RATIOS AND THE RESULTANT U-233 FISSION CROSS SECTIONS.

ENERGY (MEV)	ENERGY RESOLUTION <sup>a</sup> (MEV)	CROSS SECTION RATIO	UNCORR. ERROR (%)	TOTAL ERROR (%)	CROSS SECTION <sup>b</sup> (#)
.142	.042	1.475	.98	1.56	2.171
.153	.086	1.494	.82	2.11	2.169
.174	.040	1.518	1.11	1.58	2.152
.206	.050	1.576	.90	1.67	2.154
.256	.034	1.671	1.43	1.82	2.164
.306	.044	1.760	.95	1.27	2.215
.351	.031	1.717	1.34	1.57	2.119
.395	.040	1.741	.80	1.15	2.109
.446	.029	1.724	1.09	1.36	2.044
.495	.036	1.760	.71	1.08	2.056
.550	.027	1.734	1.07	1.35	2.002
.604	.036	1.721	.74	1.11	1.970
.661	.026	1.741	1.11	1.38	1.983
.678	.042	1.720	.63	1.04	1.958
.723	.042	1.702	1.00	1.30	1.935
.795	.062	1.703	.71	1.16	1.939
.896	.039	1.625	1.00	1.36	1.895
.995	.058	1.548	.72	1.13	1.887
1.125	.036	1.561	1.01	1.30	1.897
1.255	.034	1.564	1.01	1.30	1.913
1.300	.070	1.551	.76	1.12	1.905
1.327	.069	1.548	.83	1.17	1.906
1.416	.067	1.522	.85	1.18	1.888
1.496*	.065	1.539	.30	.87	1.925
1.777	.062	1.534	.85	1.18	1.972
1.966*-	.058	1.537	.29	.87	1.993
2.256	.110	1.533	.85	1.18	1.975
2.495*	.104	1.534	.29	.87	1.946
2.714	.100	1.522	.85	1.18	1.899
2.998*	.095	1.541	.27	.86	1.978
3.271	.089	1.532	.84	1.17	1.830
3.523	.084	1.537	.84	1.17	1.802
3.775	.080	1.524	.84	1.17	1.753
4.027	.078	1.495	.85	1.18	1.691
4.278	.077	1.479	.86	1.19	1.661
4.529	.074	1.506	.77	1.13	1.569
4.765	.292	1.472	1.05	1.34	1.598
4.780	.073	1.511	.77	1.13	1.638
5.360	.221	1.475	1.02	1.35	1.545
5.918	.190	1.565	1.08	1.36	1.703

TABLE X. THE (CONTINUED)

ENERGY (MEV)	ENERGY RESOLUTION <sup>a</sup> (MEV)	CROSS SECTION RATIO	UNCORR. ERROR (%)	TOTAL ERROR (%)	CROSS SECTION <sup>b</sup> (B)
6.357	.170	1.482	.93	1.38	1.904
6.482	.164	1.475	1.07	1.46	1.996
6.624	.157	1.433	.92	1.33	2.036
6.884	.147	1.367	.93	1.30	2.071
7.121	.140	1.344	1.04	1.36	2.150
7.169	1.380	1.348	1.01	1.33	2.181
7.399	.132	1.316	.99	1.30	2.225
7.478	.132	1.288	.88	1.21	2.206
7.653	.129	1.283	1.24	1.49	2.240
7.906	.126	1.276	1.24	1.49	2.264
8.154	.124	1.298	1.24	1.49	2.315
8.405	.122	1.297	1.41	1.64	2.312
8.651	.120	1.298	1.30	1.54	2.309
8.897	.120	1.302	1.21	1.47	2.309
9.143	.120	1.273	1.17	1.46	2.252
9.367	.120	1.288	1.24	1.52	2.273

\*Normalization points.

<sup>a</sup>Full-width-at-half-maximum.

<sup>b</sup>Based on the  $^{235}\text{U}$  fission cross section from ENDF/B-V (ref. 29).

TABLE XI. THE U-234/U-235 FISSION CROSS SECTION RATIOS AND THE RESULTANT U-234 FISSION CROSS SECTIONS.

ENERGY (MEV)	ENERGY RESOLUTION <sup>a</sup> (MEV)	CROSS SECTION RATIO	UNCORR. ERROR (%)	TOTAL ERROR (%)	CROSS SECTION <sup>b</sup> (B)
.600	.044	.682	1.06	3.67	.781
.643	.043	.785	1.16	3.11	.895
.700	.042	.891	1.15	2.59	1.014
.747	.041	1.046	1.14	2.61	1.190
.799	.040	1.172	.97	1.29	1.334
.850	.039	1.113	.99	1.58	1.276
.900	.039	1.048	.91	1.69	1.225
.946	.038	.948	1.14	1.76	1.136
.998	.038	.919	1.14	1.43	1.121
1.048	.037	.967	1.18	2.09	1.175
1.097	.037	1.011	1.14	1.63	1.229
1.148	.036	1.007	1.17	1.44	1.225
1.194	.036	1.021	.82	1.17	1.246
1.244	.035	1.017	.97	1.29	1.244
1.338	.068	1.069	.94	1.34	1.318
1.434	.067	1.098	.97	1.38	1.366
1.536	.065	1.147	.88	1.32	1.440
1.631	.062	1.196	.81	1.22	1.516
1.733	.062	1.216	.81	1.17	1.558
1.817	.061	1.227	.97	1.28	1.581
1.829	.061	1.207	1.10	1.38	1.556
1.928*	.060	1.206	.54	.99	1.561
2.242*	.111	1.177	.54	.99	1.517
2.490*	.105	1.191	.62	1.04	1.511
2.736*	.101	1.215	.48	.96	1.514
2.983*	.094	1.243	.51	1.00	1.517
3.231	.089	1.281	.92	1.25	1.535
3.482	.085	1.286	.76	1.14	1.512
3.726	.081	1.294	.76	1.16	1.493
3.973	.079	1.286	.74	1.17	1.458
4.229	.077	1.275	1.00	1.47	1.433
4.479	.075	1.326	.89	1.61	1.475
4.794	.073	1.276	1.00	1.75	1.382
4.982	.072	1.281	1.01	2.59	1.365
4.747	.296	1.270	1.06	1.34	1.381
5.048	.250	1.236	1.06	1.34	1.311
5.343	.222	1.258	1.06	1.34	1.318
5.622	.204	1.258	1.06	1.34	1.321
5.900	.190	1.229	1.06	1.34	1.331
6.168	.178	1.226	1.14	1.40	1.461

TABLE XI. THE (CONTINUED)

ENERGY (MEV)	ENERGY RESOLUTION <sup>a</sup> (MEV)	CROSS SECTION RATIO	UNCORR. ERROR (%)	TOTAL ERROR (%)	CROSS SECTION <sup>b</sup> (B)
6.435	.165	1.202	1.06	1.34	1.594
6.691	.154	1.191	1.08	1.36	1.729
6.952	.144	1.191	1.07	1.35	1.831
7.207	.137	1.208	1.08	1.36	1.972
7.460	.132	1.203	1.06	1.34	2.054
7.712	.128	1.217	1.10	1.37	2.137
7.961	.126	1.217	1.10	1.37	2.164
8.192	.124	1.202	1.08	1.36	2.144
8.210	.124	1.190	1.08	1.36	2.122
7.916	.124	1.207	1.14	1.40	2.143
8.441	.122	1.201	1.17	1.43	2.140
8.686	.120	1.203	1.23	1.48	2.139
8.931	.120	1.197	1.13	1.40	2.122
8.174	.120	1.200	1.24	1.49	2.122
9.419	.120	1.196	1.13	1.40	2.109
9.673	.121	1.180	1.15	1.42	2.073
9.905	.122	1.179	1.11	1.38	2.064

\*Normalization points.

<sup>a</sup>Full-width-at-half-maximum.

<sup>b</sup>Based on the  $^{235}\text{U}$  fission cross section from ENDF/B-V (ref. 29).

TABLE XII. THE U-236/U-235 FISSION CROSS SECTION RATIOS AND THE RESULTANT U-236 FISSION CROSS SECTIONS.

ENERGY (MEV)	ENERGY RESOLUTION <sup>a</sup> (MEV)	CROSS SECTION RATIO	UNCORR. ERROR (%)	TOTAL ERROR (%)	CROSS SECTION <sup>b</sup> (B)
.596	.045	.01233	1.17	16.10	.01413
.646	.044	.01664	1.33	17.00	.01898
.695	.042	.0591	1.30	11.10	.0672
.747	.041	.0616	1.24	8.49	.0700
.795	.040	.0982	1.87	6.56	.1118
.801	.032	.110 <sup>9</sup>	1.81	4.97	.1263
.845	.040	.1467	1.62	5.87	.1681
.852	.032	.1565	1.55	5.47	.1797
.899	.031	.2117	1.38	4.16	.2472
.948	.030	.2862	1.24	1.58	.3434
.998	.030	.2940	1.25	1.59	.3586
1.047	.029	.2940	1.36	1.68	.3573
.094	.035	.345	1.22	5.03	.419
1.097	.029	.361	1.40	4.41	.438
1.146	.072	.428	1.16	4.70	.521
1.192	.035	.485	1.87	2.49	.592
1.196	.028	.474	1.39	1.99	.578
1.240	.072	.513	.69	1.99	.628
1.338	.068	.549	.69	1.53	.676
1.434	.066	.576	.69	1.18	.716
1.534	.064	.529	.75	1.52	.664
1.631	.062	.543	.75	1.36	.689
1.727	.062	.603	.88	1.46	.772
1.823	.061	.606	.77	1.19	.782
1.925	.060	.619	.77	1.16	.801
2.023	.059	.639	.84	1.22	.830
2.243*	.110	.668	.70	1.15	.861
2.490*	.105	.687	.70	1.12	.872
2.736*	.101	.697	.70	1.11	.868
2.983*	.095	.716	.70	1.12	.874
3.230	.090	.728	.78	1.17	.872
3.477	.085	.754	.80	1.21	.887
3.725	.081	.769	.80	1.26	.888
3.976	.078	.778	.79	1.35	.882
4.228	.078	.782	.93	2.01	.880
4.479	.075	.795	.94	1.96	.885
4.731	.074	.780	.95	2.42	.849
4.747	.296	.787	.84	1.21	.956
5.048	.250	.778	.86	1.21	.925
5.343	.222	.789	.89	1.27	.926

TABLE XII. TH (CONTINUED)

ENERGY (MEV)	ENERGY RESOLUTION <sup>a</sup> (MEV)	CROSS SECTION RATIO	UNCORR. ERROR (%)	TOTAL ERROR (%)	CROSS SECTION <sup>b</sup> (B)
5.622	.204	.818	.89	1.30	.859
5.900	.190	.840	.90	1.30	.910
6.168	.178	.836	.93	1.33	.997
6.435	.165	.884	.96	1.31	1.172
6.695	.154	.908	1.03	1.34	1.319
6.952	.144	.890	1.05	1.36	1.368
7.207	.137	.884	.90	1.24	1.443
7.460	.132	.884	1.03	1.34	1.509
7.712	.128	.861	1.03	1.34	1.512
8.076	.125	.869	.99	1.30	1.549
8.340	.123	.878	.99	1.34	1.567
8.686	.120	.858	.94	1.28	1.526
8.931	.120	.864	1.06	1.42	1.532
9.174	.120	.855	1.04	1.43	1.512
9.419	.120	.862	1.05	1.50	1.520
9.673	.121	.828	1.05	1.53	1.456
9.905	.122	.867	1.03	1.78	1.519

\*Normalization points.

<sup>a</sup>Full-width-at-half-maximum.

<sup>b</sup>Based on the  $^{235}\text{U}$  fission cross section from ENDF/B-V (ref. 29).

TABLE XIII. THE U-238/U-235 FISSION CROSS SECTION RATIOS  
AND THE RESULTANT U-238 FISSION CROSS SECTIONS.

ENERGY (MEV)	ENERGY RESOLUTION <sup>a</sup> (MEV)	CROSS SECTION RATIO	UNCORR. ERROR (%)	TOTAL ERROR (%)	CROSS SECTION <sup>b</sup> (R)
.899	.023	.00997	3.72	3.86	.01164
1.007	.022	.01267	2.34	3.54	.01545
1.095	.022	.02187	3.10	3.66	.02658
1.110	.022	.02132	1.91	2.70	.02591
1.146	.021	.02776	3.25	3.64	.03375
1.207	.021	.02912	1.91	3.21	.03554
1.249	.021	.0336	1.56	4.02	.0412
1.295	.028	.0511	1.53	6.55	.0627
1.353	.021	.0829	2.55	5.25	.1023
1.387	.020	.1173	2.04	4.63	.1452
1.397	.028	.1323	1.11	5.97	.1639
1.404	.020	.1528	1.24	4.32	.1894
.451	.020	.2041	1.70	5.02	.2542
1.491	.027	.2717	1.16	2.97	.3397
1.517	.020	.2721	1.04	1.82	.3411
1.548	.020	.305	1.54	2.12	.383
1.591	.027	.317	.99	1.77	.401
1.620	.019	.325	.99	1.70	.411
1.694	.020	.330	1.55	2.08	.422
1.694	.027	.360	.97	1.70	.460
1.753	.019	.353	1.54	2.03	.453
1.724	.019	.338	.99	1.67	.433
1.794	.026	.371	1.00	1.66	.478
1.826	.019	.388	1.00	1.59	.501
1.854	.019	.372	1.46	1.88	.480
1.896	.026	.399	.93	1.45	.516
1.918	.019	.400	1.10	1.53	.518
1.985	.032	.415	.94	1.45	.539
1.992	.115	.407	.49	1.02	.528
2.000	.019	.393	1.08	1.47	.510
2.044	.114	.421	.91	1.34	.546
2.197	.102	.424	.88	1.31	.547
2.500*	.104	.428	.35	.83	.543
2.890*	.097	.428	.35	.83	.527
3.256*	.089	.446	.28	.87	.533
3.476	.085	.464	.86	1.49	.546
3.484	.085	.466	.55	1.14	.548
3.575	.097	.467	.78	1.24	.545
3.570	.080	.480	.86	1.27	.556
3.376	.078	.488	.86	1.39	.557

TABLE XIII. T (CONTINUED)

ENERGY (MEV)	ENERGY RESOLUTION <sup>a</sup> (MEV)	CROSS SECTION R4TTO	UNCORR. ERROR (%)	TOTAL ERROR (%)	CROSS SECTION <sup>b</sup> (B)
3.992	.078	.495	.94	1.67	.561
4.992	.072	.515	.47	4.53	.549
4.475	.082	.506	.71	1.69	.564
4.078	.085	.490	.57	1.18	.553
4.075	.078	.495	.86	1.60	.559
5.083	.082	.517	.84	1.24	.548
5.147	.071	.516	.74	5.28	.545
5.334	.070	.526	1.05	1.39	.551
5.439	.216	.524	.82	1.32	.548
5.622	.204	.538	.73	1.31	.565
5.826	.191	.565	.73	1.35	.605
6.168	.178	.573	.74	1.42	.683
6.430	.165	.620	.72	1.27	.821
6.692	.154	.617	.74	1.23	.896
6.949	.144	.618	.67	1.19	.949
7.204	.137	.606	.75	1.25	.989
7.457	.132	.606	.68	1.21	1.035
7.709	.128	.584	.75	1.25	1.025
7.960	.126	.576	.74	1.24	1.025
8.208	.124	.570	.80	1.27	1.017
8.455	.122	.571	.67	1.21	1.018
8.699	.120	.567	.78	1.33	1.008
8.946	.121	.580	.75	1.42	1.028
9.191	.120	.578	.71	1.51	1.022
9.433	.121	.589	.74	1.68	1.038
9.675	.121	.583	.76	1.81	1.025
9.818	.122	.591	.76	1.87	1.037
10.160	.124	.570	.77	1.86	0.995
10.400	.126	.554	.76	1.73	0.964

\*Normalization points.

<sup>a</sup>Full-width-at-half-maximum.

<sup>b</sup>Based on the  $^{235}\text{U}$  fission cross section from ENDF/B-V (ref. 29).

TABLE XIV. THE NP-237/U-235 FISSION CROSS SECTION RATIOS  
AND THE RESULTANT NP-237 FISSION CROSS SECTIONS.

ENERGY (MEV)	ENERGY RESOLUTION <sup>a</sup> (MEV)	CROSS SECTION RATIO	UNCORR. ERROR (%)	TOTAL ERROR (%)	CROSS SECTION <sup>b</sup> ( $\mu$ )
.131	.062	.01180	3.31	4.31	.1765
.234	.060	.02610	3.34	5.39	.3452
.286	.056	.0376	3.71	5.53	.477
.335	.056	.0642	2.71	4.34	.798
.387	.054	.1157	2.31	3.95	.406
.438	.052	.2222	1.12	2.88	.644
.489	.052	.345	83	2.24	.404
.540	.050	.479	75	1.80	.554
.641	.048	.765	82	1.45	.873
.692	.048	.872	69	1.23	.992
.741	.048	.989	81	1.30	1.125
.792	.048	1.069	75	1.23	1.217
.842	.046	1.142	76	1.21	1.308
.873	.078	1.151	64	1.16	1.331
.923	.076	1.172	69	1.18	1.387
.973	.076	1.207	65	1.15	1.465
.994	.076	1.206	69	1.16	1.470
1.074	.074	1.212	66	1.13	1.473
1.094	.072	1.223	60	1.09	1.486
1.175	.072	1.233	70	1.14	1.502
1.195	.072	1.242	65	1.11	1.515
1.276	.070	1.276	69	1.12	1.564
1.296	.068	1.270	62	1.08	1.559
1.377	.070	1.284	68	1.11	1.588
1.397	.068	1.280	71	1.13	1.586
1.497	.064	1.294	68	1.11	1.619
1.598	.062	1.309	67	1.11	1.654
1.698	.062	1.307	66	1.11	1.670
1.799	.060	1.311	67	1.11	1.688
1.910	.060	1.331	67	1.11	1.723
1.921	.116	1.316	68	1.11	1.704
2.000	.060	1.306	66	1.10	1.695
2.022	.114	1.316	70	1.12	1.708
2.122*	.112	1.330	27	.92	1.723
2.223*	.110	1.336	27	.92	1.724
2.326*	.108	1.327	27	.92	1.704
2.425*	.106	1.317	26	.92	1.680
2.526*	.104	1.325	27	.92	1.677
2.926	.096	1.360	67	1.11	1.668
3.125	.092	1.360	63	1.08	1.643

TABLE XIV. TH (CONTINUED)

ENERGY (MEV)	ENERGY RESOLUTION <sup>a</sup> (MEV)	CROSS SECTION RATIO	UNCORR. ERROR (%)	TOTAL ERROR (%)	CROSS SECTION <sup>b</sup> (R)
3.328	.088	1.362	.60	1.07	1.621
3.527	.084	1.393	.64	1.09	1.633
3.727	.080	1.389	.60	1.07	1.603
3.927	.080	1.388	.62	1.08	1.579
4.127	.076	1.367	.66	1.10	1.541
4.335	.076	1.389	.64	1.09	1.558
4.525	.074	1.420	.68	1.11	1.574
4.615	.314	1.375	.90	1.26	1.513
4.923	.268	1.390	.94	1.29	1.489
5.234	.232	1.374	.95	1.31	1.444
5.516	.210	1.391	.92	1.33	1.457
5.793	.196	1.465	.98	1.37	1.561
6.070	.182	1.500	.91	1.29	1.718
6.338	.172	1.477	.88	1.24	1.884
6.610	.158	1.415	.88	1.34	2.002
6.867	.148	1.382	.68	1.17	2.087
7.125	.140	1.341	.68	1.14	2.148
7.387	.134	1.319	.68	1.12	2.226
7.683	.130	1.307	.67	1.12	2.289
7.893	.126	1.290	.67	1.12	2.288
8.141	.124	1.267	.66	1.11	2.260
8.392	.122	1.263	.65	1.10	2.252
8.638	.120	1.207	1.22	1.51	2.148
8.884	.120	1.231	.97	1.31	2.184
9.127	.120	1.224	.96	1.30	2.166
9.374	.120	1.226	.96	1.30	2.163

\*Normalization points.

<sup>a</sup>Full-width-at-half-maximum.

<sup>b</sup>Based on the  $^{235}\text{U}$  fission cross section from ENDF/B-V (ref. 29).

TABLE XV. THE PU-239/U-235 FISSION CROSS SECTION RATIOS AND THE RESULTANT PU-239 FISSION CROSS SECTIONS.

ENERGY (MEV)	ENERGY RESOLUTION <sup>a</sup> (MEV)	CROSS SECTION RATIO	UNCORR. ERROR (%)	TOTAL ERROR (%)	CROSS SECTION <sup>b</sup> (B)
.146	.020	.968	.90	1.28	1.417
.172	.019	1.107	1.28	1.57	1.572
.197	.019	1.094	.90	1.29	1.511
.220	.018	1.131	1.34	1.62	1.519
.247	.017	1.157	.88	1.25	1.510
.268	.017	1.215	1.28	1.56	1.559
.268	.058	1.191	.99	1.62	1.529
.294	.022	1.266	1.34	1.62	1.602
.311	.016	1.260	1.38	1.63	1.583
.323	.066	1.264	.99	1.65	1.580
.336	.016	1.256	1.42	1.66	1.561
.348	.016	1.308	1.46	1.69	1.617
.384	.062	1.286	.98	1.46	1.565
.391	.062	1.340	1.49	1.83	1.625
.452	.060	1.346	.94	1.36	1.592
.500	.046	1.372	.91	1.28	1.601
.550	.045	1.393	.94	1.27	1.609
.598	.055	1.428	.80	1.22	1.635
.650	.054	1.418	1.04	1.40	1.616
.687	.053	1.422	1.71	1.95	1.618
.746	.052	1.480	1.05	1.37	1.683
.795	.050	1.546	1.81	2.00	1.760
.846	.049	1.511	1.06	1.39	1.732
.877	.080	1.499	1.86	2.11	1.736
.943	.047	1.431	1.51	1.74	1.712
.980	.047	1.432	1.49	1.70	1.743
.993	.046	1.472	.94	1.25	1.794
1.045	.045	1.416	1.77	1.95	1.721
1.099	.044	1.443	.93	1.26	1.753
1.140	.074	1.480	.95	1.32	1.799
1.196	.043	1.467	.93	1.25	1.789
1.234	.072	1.497	.95	1.34	1.829
1.332	.070	1.559	.95	1.31	1.921
1.429	.067	1.603	1.41	1.64	1.992
1.526	.065	1.581	1.41	1.64	1.984
1.622	.063	1.544	1.45	1.36	1.957
1.720	.061	1.503	1.43	1.65	1.924
1.818	.059	1.555	1.47	1.68	2.005
1.893	.120	1.550	1.19	1.44	2.005
1.924	.056	1.551	1.46	1.67	2.009

TABLE XV. THE (CONTINUED)

ENERGY (MEV)	ENERGY RESOLUTION <sup>a</sup> (MEV)	CROSS SECTION RATIO	UNCORR. ERROR (%)	TOTAL ERROR (%)	CROSS SECTION <sup>b</sup> (R)
2.021*	.054	1.609	1.74	1.92	2.089
2.232*	.111	1.554	.68	1.07	2.005
2.476*	.106	1.518	.67	1.06	1.929
2.792*	.101	1.532	.74	1.10	1.901
2.975*	.096	1.543	.57	1.00	1.885
3.226	.092	1.544	.86	1.19	1.851
3.470	.087	1.580	.75	1.11	1.861
3.719	.083	1.581	.72	1.10	1.826
3.968	.080	1.568	.74	1.11	1.779
4.221	.076	1.579	1.03	1.33	1.776
4.472	.074	1.573	1.11	1.39	1.752
4.724	.074	1.607	1.06	1.36	1.752
4.972	.070	1.607	1.23	1.51	1.715
5.714	.308	1.619	.87	1.20	1.766
5.017	.264	1.625	.92	1.24	1.728
5.309	.235	1.640	.88	1.21	1.718
5.594	.211	1.663	.99	1.29	1.744
5.867	.196	1.663	.96	1.35	1.791
6.137	.180	1.609	.99	1.52	1.894
6.401	.172	1.514	1.01	1.50	1.978
6.660	.163	1.430	1.04	1.42	2.056
6.921	.154	1.388	1.07	1.41	2.120
7.176	.146	1.372	1.01	1.33	2.224
7.432	.142	1.319	.99	1.29	2.243
7.686	.138	1.312	.94	1.25	2.299
7.936	.133	1.301	.97	1.27	2.313
8.182	.132	1.363	1.00	1.29	2.431
8.428	.131	1.316	.99	1.29	2.347
8.673	.131	1.315	.99	1.29	2.340
8.918	.131	1.325	1.02	1.32	2.351
9.161	.132	1.307	1.03	1.35	2.313
9.407	.133	1.344	.99	1.33	2.370
9.648	.137	1.317	.97	1.36	2.316
9.903	.142	1.308	.99	1.55	2.288

\*Normalization points.

<sup>a</sup>Full-width-at-half-maximum.

<sup>b</sup>Based on the  $^{235}\text{U}$  fission cross section from ENDF/B-V (ref. 29).

TABLE XVI. THE PU-240/U-235 FISSION CROSS SECTION RATIOS  
AND THE RESULTANT PU-240 FISSION CROSS SECTIONS.

ENERGY (MEV)	ENERGY RESOLUTION <sup>a</sup> (MEV)	CROSS SECTION RATIO	UNCORR. ERROR (%)	TOTAL ERROR (%)	CROSS SECTION <sup>b</sup> (B)
.335	.062	.1121	4.09	5.73	.1394
.393	.060	.1554	3.08	7.39	.1884
.450	.058	.2242	2.07	7.31	.2655
.506	.056	.334	1.75	8.17	.389
.560	.054	.470	1.71	6.79	.542
.616	.053	.612	1.65	4.71	.700
.669	.051	.728	1.65	3.44	.830
.715	.060	.803	1.64	3.35	.913
.768	.058	.926	1.64	2.82	1.052
.821	.058	1.028	1.65	2.56	1.173
.873	.056	1.122	1.64	2.36	1.298
.925	.055	1.163	1.65	2.27	1.378
.979	.055	1.198	1.65	2.19	1.457
1.030	.053	1.185	1.65	1.98	1.442
1.074	.072	1.232	1.70	2.02	1.497
1.178	.072	1.207	1.71	2.02	1.470
1.281	.070	1.238	1.71	2.01	1.518
1.385	.068	1.239	1.71	2.01	1.533
1.488	.066	1.228	1.71	2.01	1.535
1.590	.064	1.259	1.71	2.01	1.590
1.692	.062	1.273	1.71	2.01	1.625
1.762	.121	1.241	1.66	1.97	1.594
1.856	.118	1.266	1.66	1.97	1.635
1.926	.117	1.287	1.61	1.93	1.667
2.061*	.113	1.313	1.63	1.23	1.703
2.322*	.109	1.312	1.64	1.23	1.685
2.566*	.102	1.320	1.64	1.23	1.666
2.803*	.099	1.348	1.64	1.23	1.671
2.935	.096	1.366	1.58	1.90	1.674
3.046*	.093	1.395	1.62	1.23	1.694
3.228	.088	1.404	1.63	1.95	1.683
3.552	.084	1.451	1.64	1.97	1.697
3.793	.080	1.413	1.65	2.01	1.623
4.046	.078	1.437	1.66	2.02	1.624
4.308	.076	1.403	1.70	2.11	1.574
4.559	.075	1.432	1.70	2.20	1.583
4.760	.072	1.443	1.81	2.09	1.567
5.220	.233	1.430	1.71	2.01	1.503
5.510	.211	1.457	1.71	2.01	1.526
5.791	.195	1.467	1.77	2.06	1.562

TABLE XVI. TH (CONTINUED)

ENERGY (MEV)	ENERGY RESOLUTION <sup>a</sup> (MEV)	CROSS SECTION RATIO	UNCORR. ERROR (%)	TOTAL ERROR (%)	CROSS SECTION <sup>b</sup> (B)
6.066	.183	1.440	1.73	2.06	1.646
6.337	.170	1.379	1.73	2.06	1.758
6.610	.158	1.344	1.69	2.00	1.901
6.866	.147	1.326	1.73	2.03	2.002
7.125	.139	1.311	1.76	2.05	2.099
7.382	.134	1.290	1.75	2.04	2.175
7.635	.129	1.264	1.74	2.03	2.203
7.888	.126	1.233	1.73	2.02	2.187
8.143	.124	1.227	1.72	2.02	2.189
8.387	.122	1.249	1.73	2.02	2.227
8.605	.120	1.251	1.75	2.04	2.226
8.860	.120	1.250	1.80	2.08	2.218
9.128	.120	1.235	1.84	2.12	2.185
9.351	.121	1.250	1.84	2.12	2.206
9.597	.121	1.237	1.80	2.08	2.176

\*Normalization points.

<sup>a</sup>Full-width-at-half-maximum.

<sup>b</sup>Based on the  $^{235}\text{U}$  fission cross section from ENDF/B-V (ref. 29).

TABLE XVII. THE PU-242/U-235 FISSION CROSS SECTION RATIOS  
AND THE RESULTANT PU-242 FISSION CROSS SECTIONS.

ENERGY (MEV)	ENERGY RESOLUTION <sup>a</sup> (MEV)	CROSS SECTION RATIO	UNCORR. ERROR (%)	TOTAL ERROR (%)	CROSS SECTION <sup>b</sup> (R)
.397	.051	.0875	3.22	10.25	.1060
.446	.049	.1234	2.90	8.52	.1463
.495	.047	.1817	2.30	8.52	.2123
.545	.046	.2432	1.96	5.74	.2812
.592	.045	.312	1.82	4.85	.358
.693	.042	.483	1.52	4.44	.549
.791	.040	.710	1.90	3.48	.808
.889	.039	.954	1.18	2.25	1.110
.987	.038	1.113	1.22	1.87	1.355
1.156	.036	1.282	1.02	1.50	1.559
1.233	.071	1.131	1.03	2.50	1.382
1.330	.068	1.164	1.02	1.66	1.433
1.429	.067	1.117	1.03	1.48	1.387
1.528	.065	1.096	.99	1.43	1.375
1.626	.063	1.126	1.01	1.45	1.427
1.772	.062	1.104	1.03	1.45	1.418
1.821	.061	1.104	1.03	1.45	1.423
1.920	.060	1.132	1.03	1.45	1.465
1.984*	.118	1.133	.38	1.09	1.469
2.241*	.110	1.101	.39	1.09	1.419
2.490*	.105	1.092	.41	1.11	1.386
2.736*	.100	1.098	.39	1.09	1.368
2.982*	.095	1.133	.38	1.11	1.383
3.231	.090	1.138	1.10	1.50	1.363
3.480	.085	1.148	2.02	1.41	1.350
3.726	.081	1.125	1.01	1.46	1.298
3.972	.079	1.147	1.33	1.72	1.300
4.479	.075	1.093	1.06	1.65	1.216
4.623	.295	1.101	1.09	1.49	1.210
4.728	.074	1.109	.96	1.74	1.208
5.025	.254	1.094	1.06	1.48	1.162
5.320	.223	1.142	1.06	1.66	1.196
5.603	.205	1.216	1.05	1.70	1.275
5.963	.187	1.265	1.06	1.59	1.393
6.150	.177	1.348	1.15	1.55	1.595
6.415	.166	1.284	1.14	1.61	1.688
6.676	.154	1.262	1.15	1.60	1.823
6.937	.145	1.209	1.06	1.52	1.952
7.193	.137	1.175	1.17	1.57	1.912
7.449	.132	1.125	1.12	1.52	1.917

TABLE XVII. T (CONTINUED)

ENERGY (MEV)	ENERGY RESOLUTION <sup>a</sup> (MEV)	CROSS SECTION RATIO	UNCORR. ERROR (%)	TOTAL ERROR (%)	CROSS SECTION <sup>b</sup> (#)
7.701	.128	1.122	1.12	1.52	1.968
7.953	.126	1.117	1.05	1.46	1.986
8.201	.124	1.105	1.10	1.50	1.971
8.013	.066	606.472	.61	.60	507.663
8.696	.120	1.091	1.20	1.57	1.939
8.940	.120	1.085	1.20	1.57	1.923
9.185	.120	1.107	1.14	1.53	1.957
9.431	.120	1.095	1.14	1.53	1.930
9.673	.121	1.084	1.14	1.53	1.904
9.923	.122	1.078	1.20	1.59	1.887

\*Normalization points.

<sup>a</sup>Full-width-at-half-maximum.

<sup>b</sup>Based on the  $^{235}\text{U}$  fission cross section from ENDF/B-V (ref. 29).

Table XVIII. The Effect of Changes in Secondary Data on the Fission Cross Section Ratio<sup>a</sup>

Q	k									
	$\frac{230}{235}$	$\frac{232}{235}$	$\frac{233}{235}$	$\frac{234}{235}$	$\frac{236}{235}$	$\frac{238}{235}$	$\frac{237}{235}$	$\frac{239}{235}$	$\frac{240}{235}$	$\frac{242}{235}$
<b>Half-lives</b>										
$^{233}\text{U}$	-	-	-0.08	+0.12	-0.25	-	+0.25	-	-	-0.10
$^{234}\text{U}$	+0.50	+0.50	+0.17	-0.12	+0.12	-	+0.38	+0.25	+0.33	+0.17
$^{236}\text{U}$	-				-0.50					
$^{237}\text{Np}$	-	-	-	-	-	-	-1.0	-	-	-
$^{239}\text{Pu}$	-	-	-	-	-	-	-	-0.50	-	-0.30
$^{240}\text{Pu}$	-	-	-	-	-	-	-	-	-	-
$^{242}\text{Pu}$	-	-	-	-	-	-	-	-	+0.33	-0.30
<b>Thermal Fission Ratios</b>										
$^{230}\text{U}/^{235}\text{U}$	-	-	+0.5	-	-	-	-	-	-	-
$^{239}\text{Pu}/^{235}\text{U}$	-	-	-	-	-	-	-	+0.5	+0.33	+0.38
<b>"Standard" Samples<sup>b</sup></b>										
<b>masses</b>										
5-1, 5-2	+1.0	+1.0	+0.06	-	-	-	+0.25	+1.0	+1.0	+0.1
SST-5, SST-1	-	-	+0.06	-	-	-	+0.50	-	-	+0.2
14	-		+0.06	+0.12	+0.25		+0.25	-	-	+0.2
3	-	-	-	-	-	-	-	-	-	-

<sup>a</sup>The relation of the secondary data, Q on the fission cross section ratio R, in  $dR/R = k dQ/Q$ .

<sup>b</sup>Changes in the "standard" samples must be due to causes other than half-lives.

Table XIX. The Percentage Change in the Normalization of the Revised Fission Cross Section Ratios

Ratio	Normalization Change
$^{230}\text{Th}/^{235}\text{U}$	+0.13
$^{232}\text{Th}/^{235}\text{U}$	-0.47
$^{233}\text{U}/^{235}\text{U}$	-1.77
$^{234}\text{U}/^{235}\text{U}$	-1.19
$^{236}\text{U}/^{235}\text{U}$	-0.01
$^{238}\text{U}/^{235}\text{U}$	-1.02
$^{237}\text{Np}/^{235}\text{U}$	0.0
$^{239}\text{Pu}/^{235}\text{U}$	+1.85
$^{240}\text{Pu}/^{235}\text{U}$	-0.09
$^{242}\text{Pu}/^{235}\text{U}$	-0.47

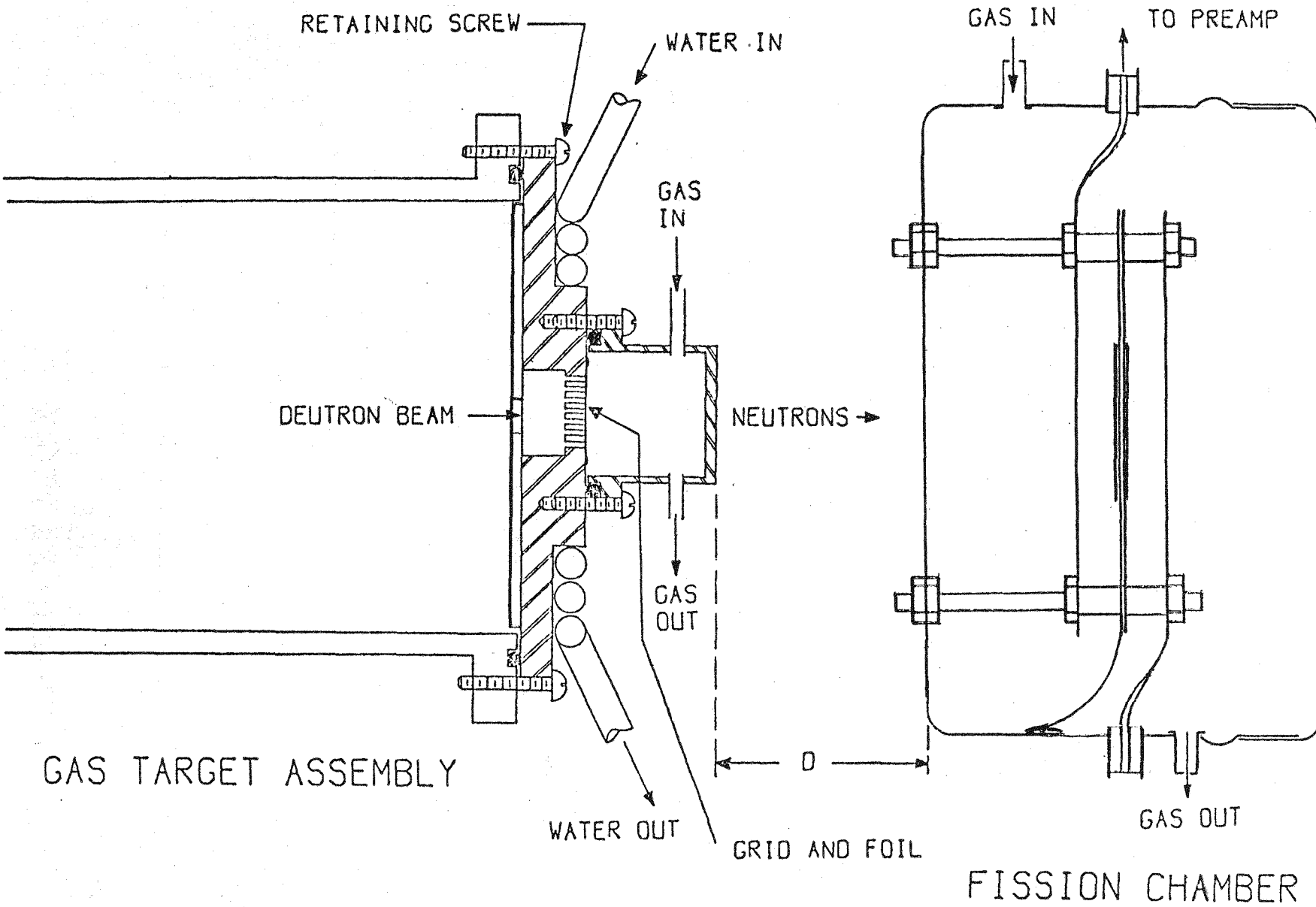


Fig. 1. The experimental set-up showing the fission chamber and gas target assembly.

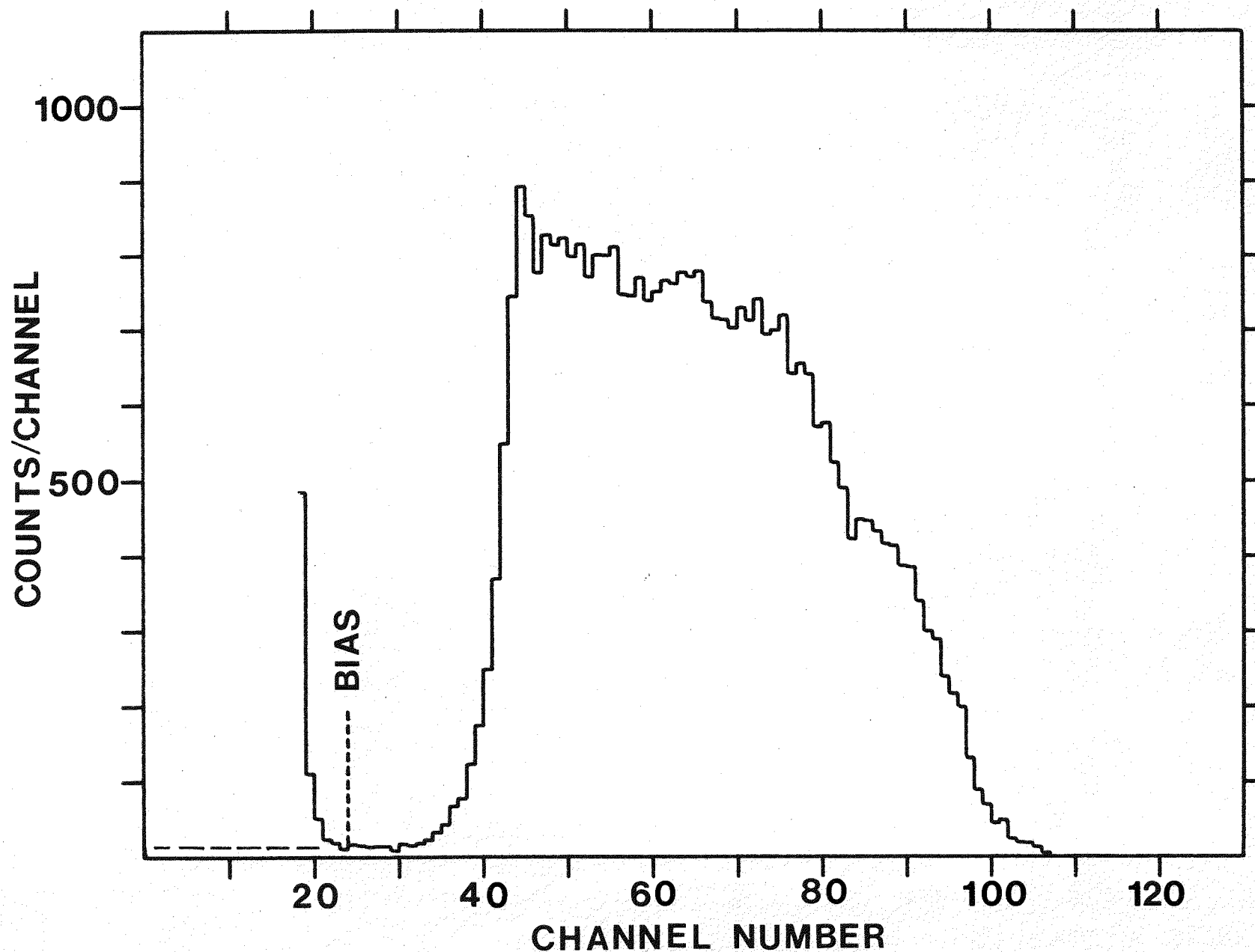


Fig. 2. A pulse-height distribution for  $^{233}\text{U}$ . The dashed line illustrates the extrapolation to channel zero.

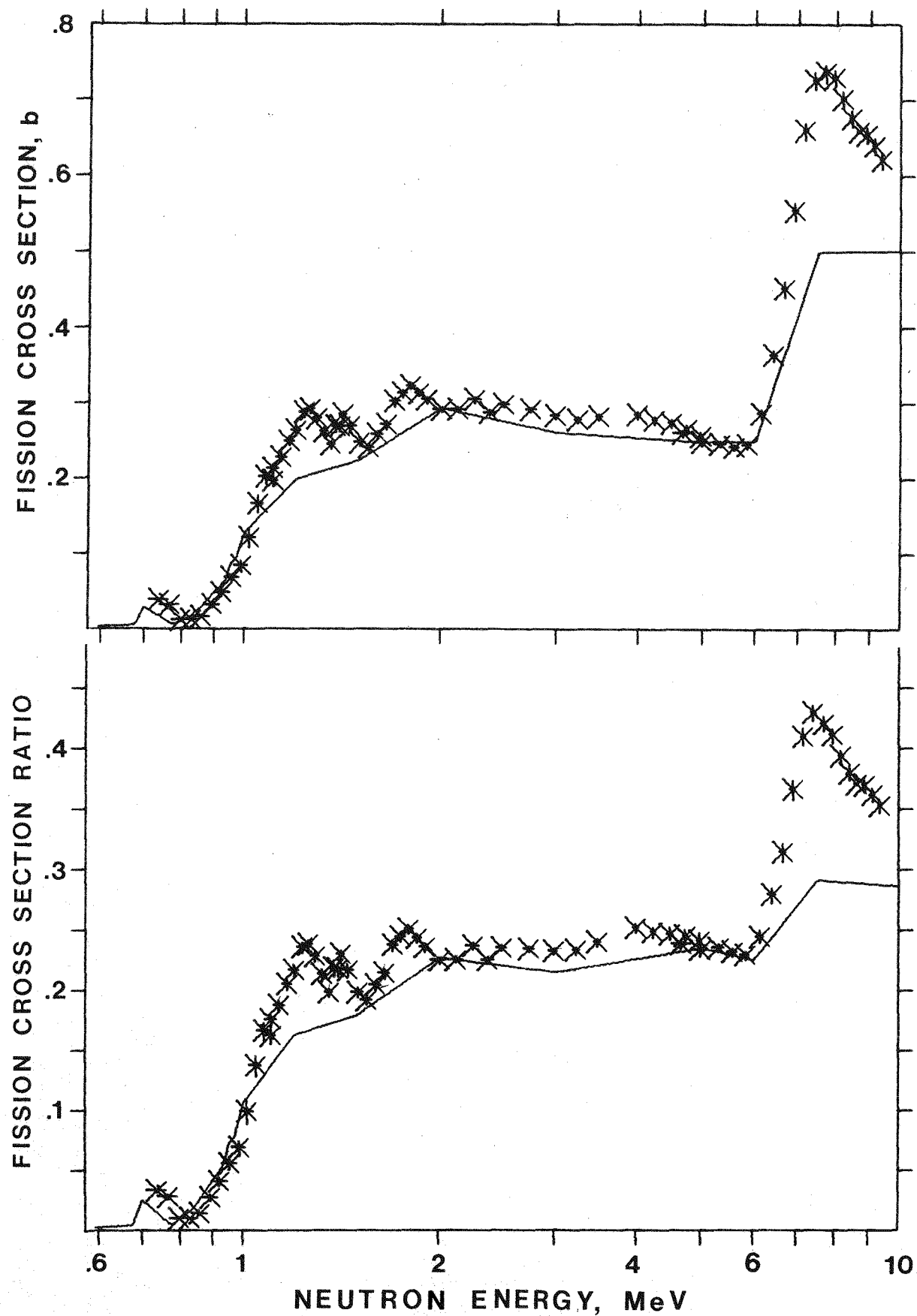


Fig. 3. The  $^{230}\text{Th}/^{235}\text{U}$  fission cross section ratios and resultant  $^{230}\text{Th}$  fission cross section. The solid line is from ENDF/B-V.

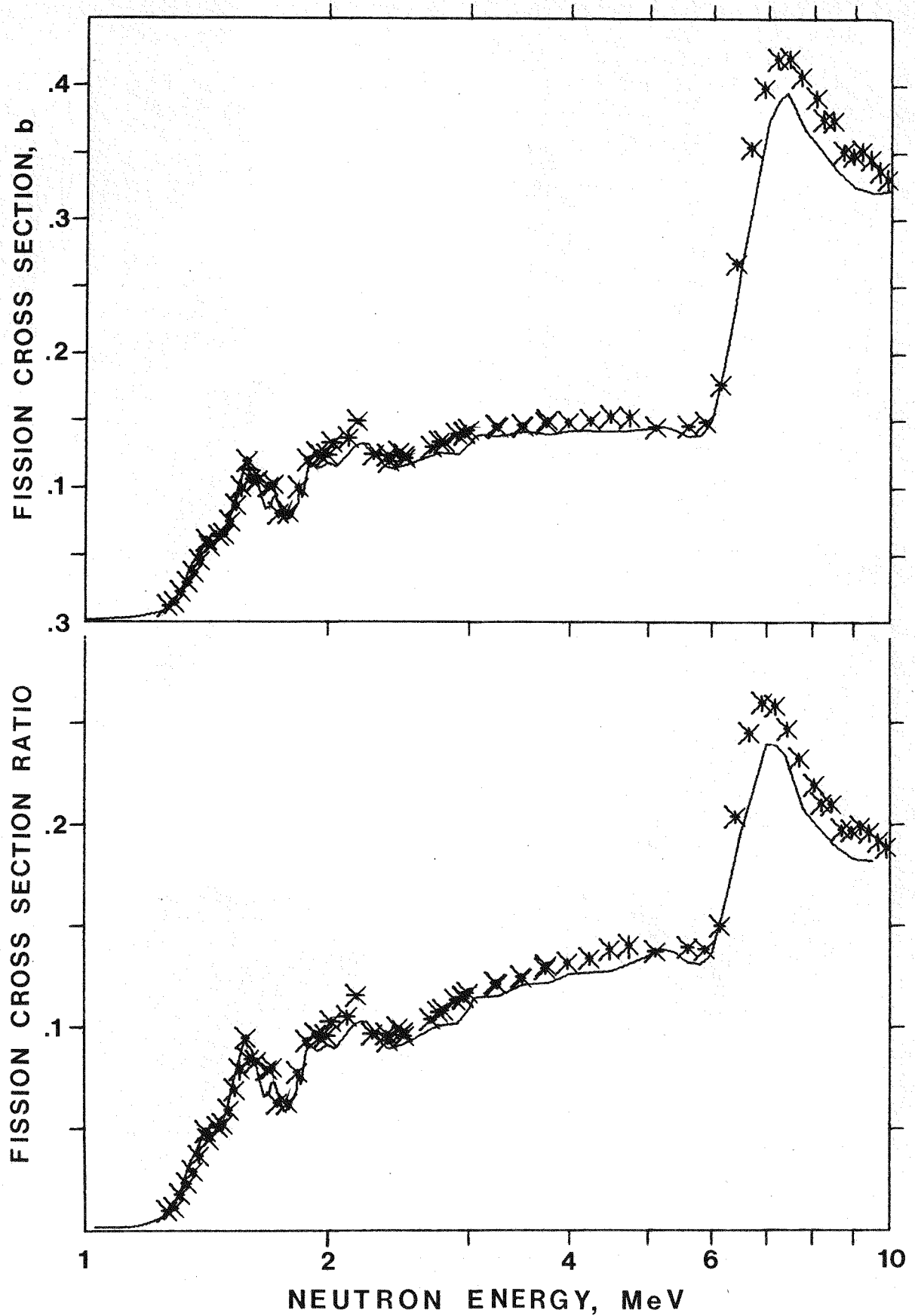


Fig. 4. The  $^{233}\text{Th}/^{235}\text{U}$  fission cross section ratios and resultant  $^{232}\text{Th}$  fission cross sections. The solid line is from ENDF/B-V.

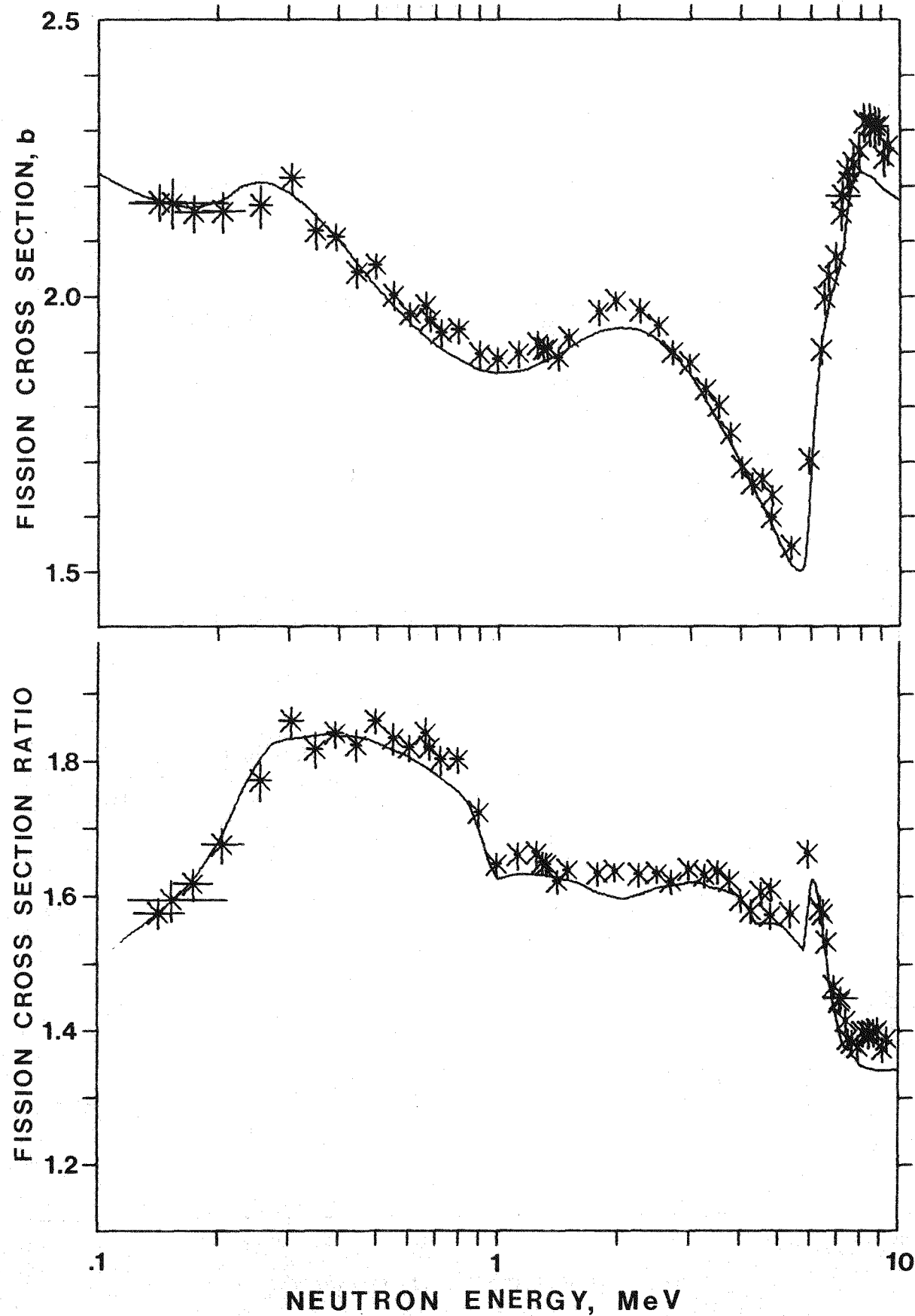


Fig. 5. The  $^{233}\text{U}/^{235}\text{U}$  fission cross section ratios and resultant  $^{233}\text{U}$  fission cross sections. The solid line is from ENDF/B-V.

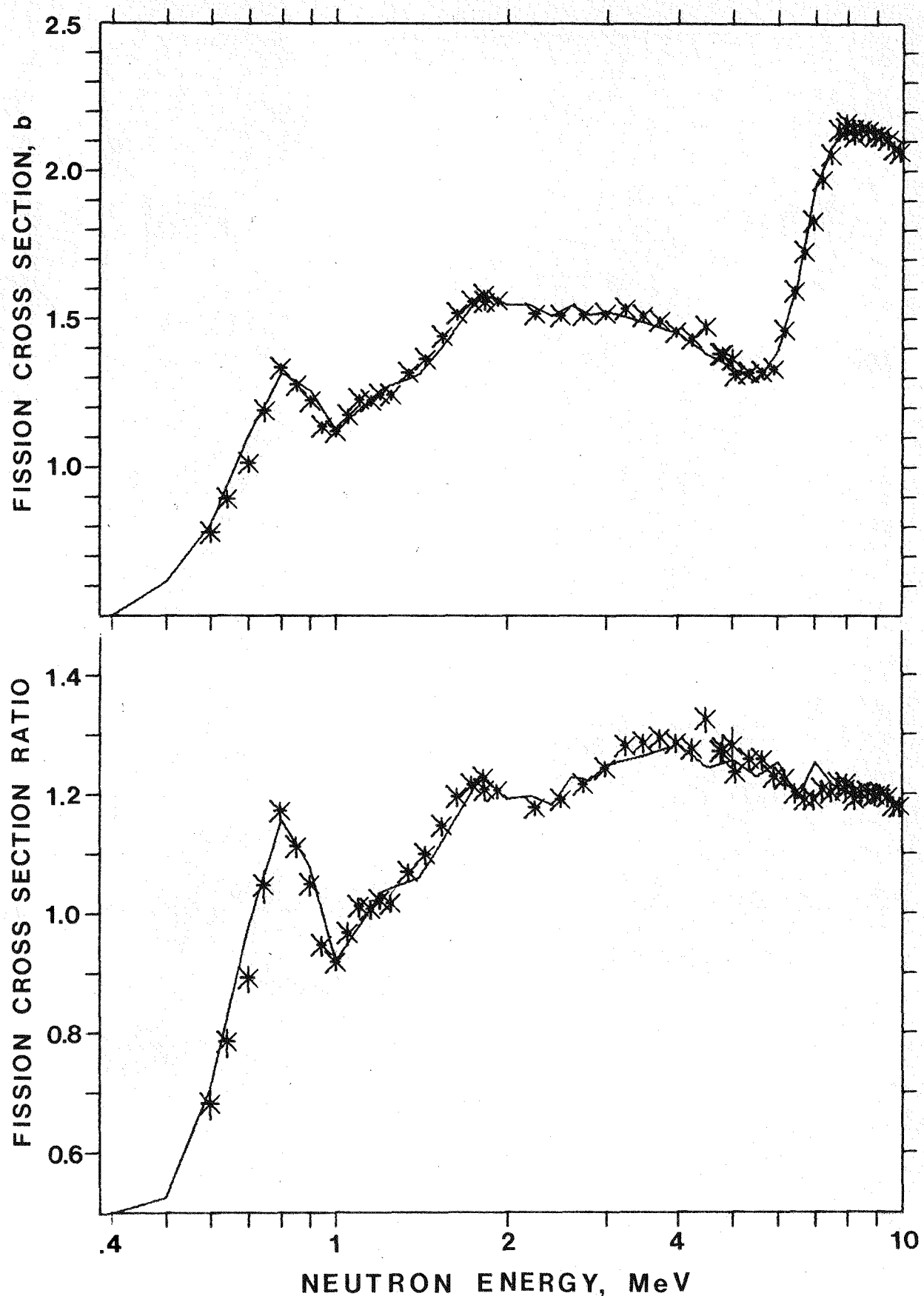


Fig. 6. The  $^{234}\text{U}/^{235}\text{U}$  fission cross section ratios and resultant  $^{234}\text{U}$  fission cross sections. The solid line is from ENDF/B-V.

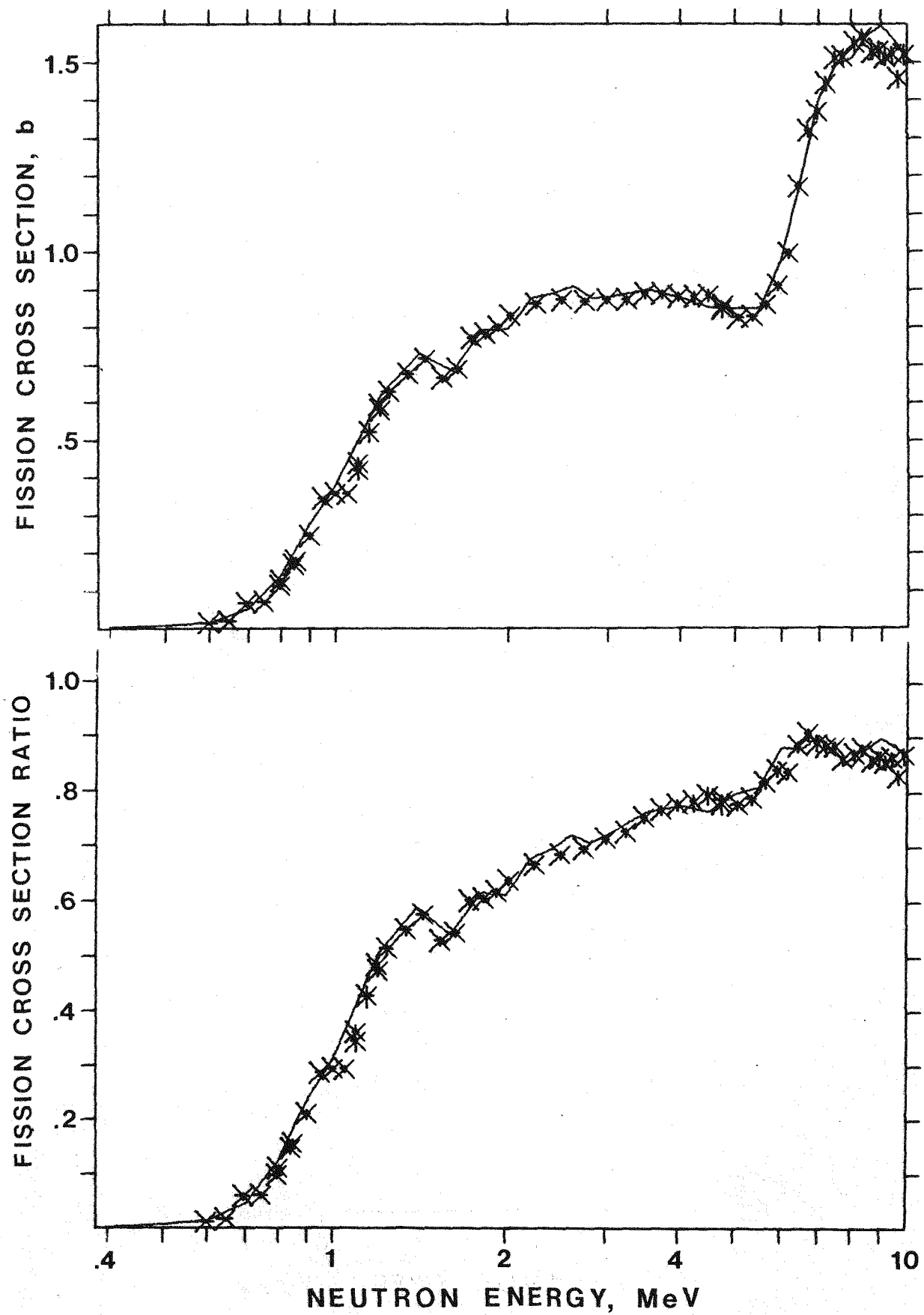


Fig. 7. The  $^{236}\text{U}/^{235}\text{U}$  fission cross section ratios and resultant  $^{236}\text{U}$  fission cross sections. The solid line is from ENDF/B-V.

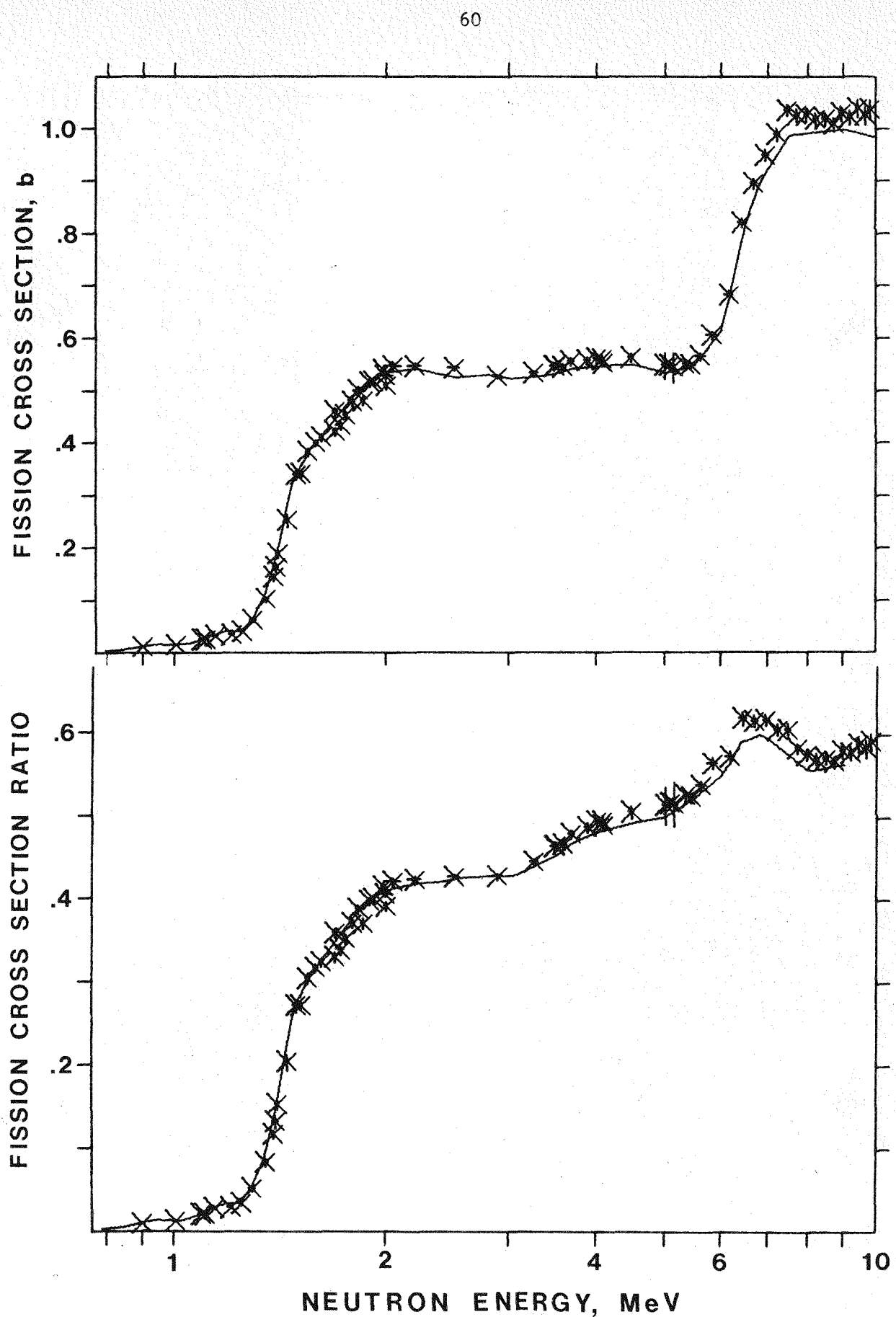


Fig. 8. The  $^{238}\text{U}/\text{U}^{235}$  fission cross section ratios and resultant  $^{238}\text{U}$  fission cross sections. The solid line is from ENDF/B-V.

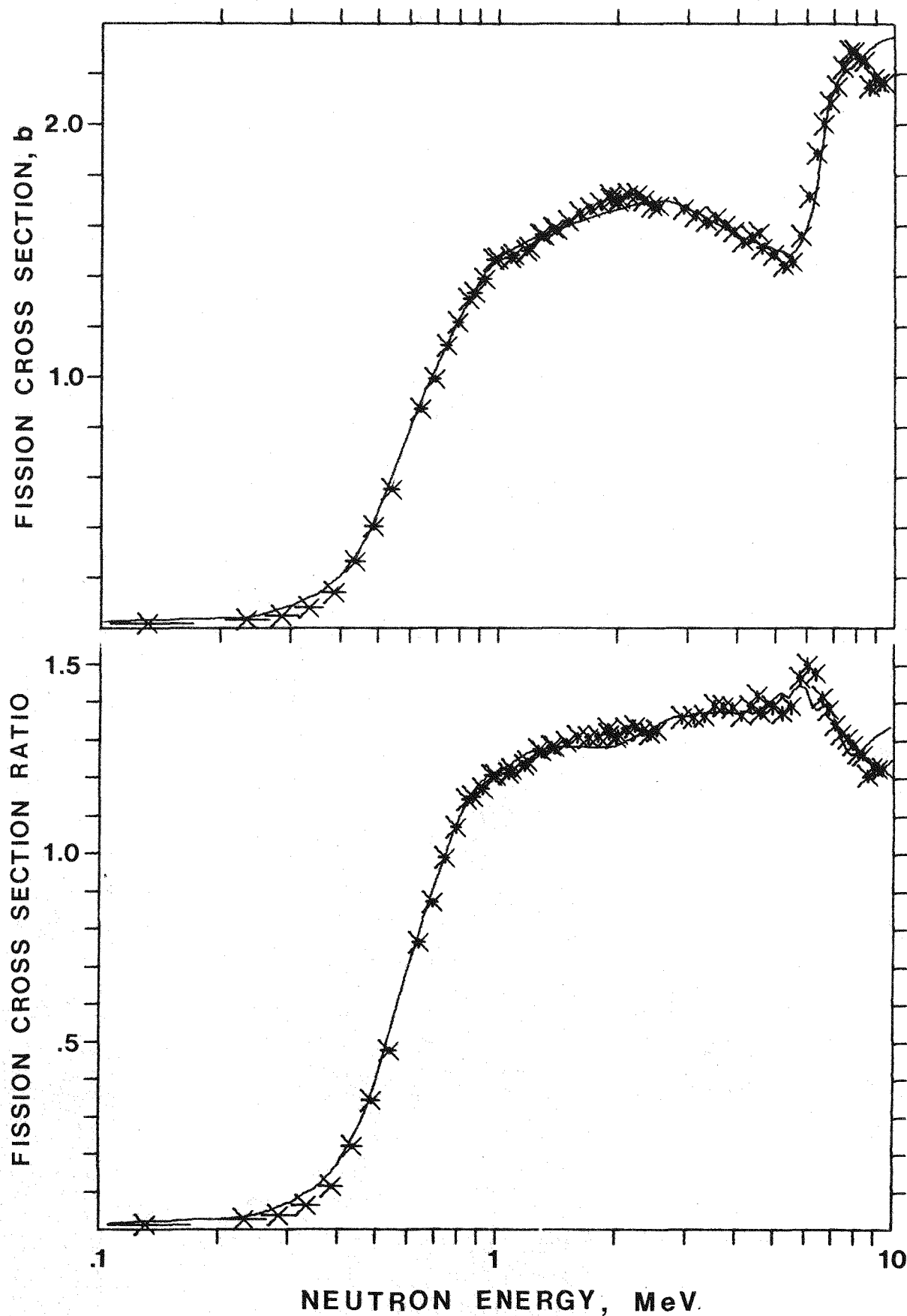


Fig. 9. The  $^{237}\text{Np}/^{235}\text{U}$  fission cross section ratios and resultant  $^{237}\text{U}$  fission cross sections. The solid line is from ENDF/B-V.

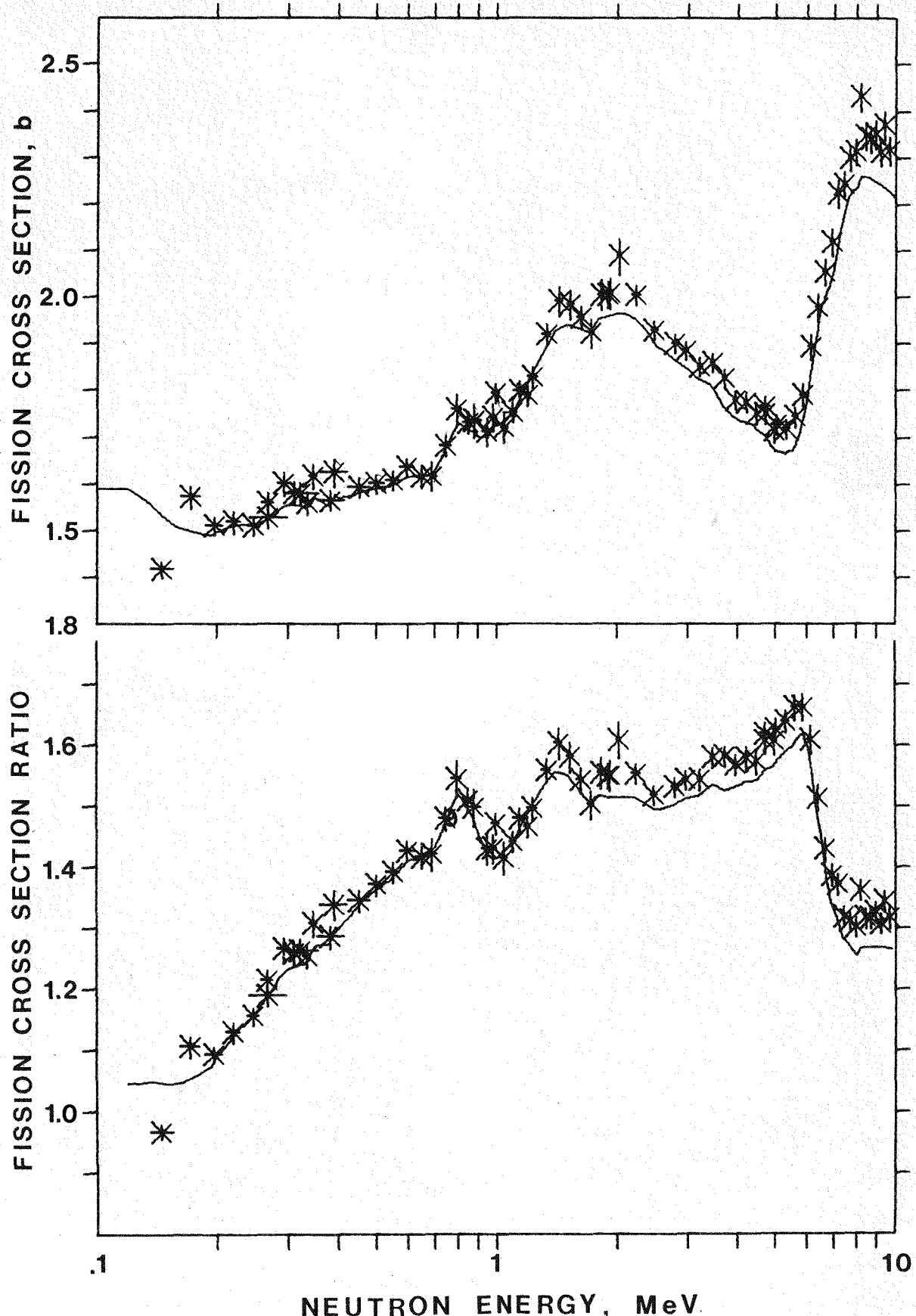


Fig. 10. The  $^{239}\text{Pu}/^{235}\text{U}$  fission cross section ratios and resultant  $^{239}\text{Pu}$  fission cross sections. The solid line is from ENDF/B-V.

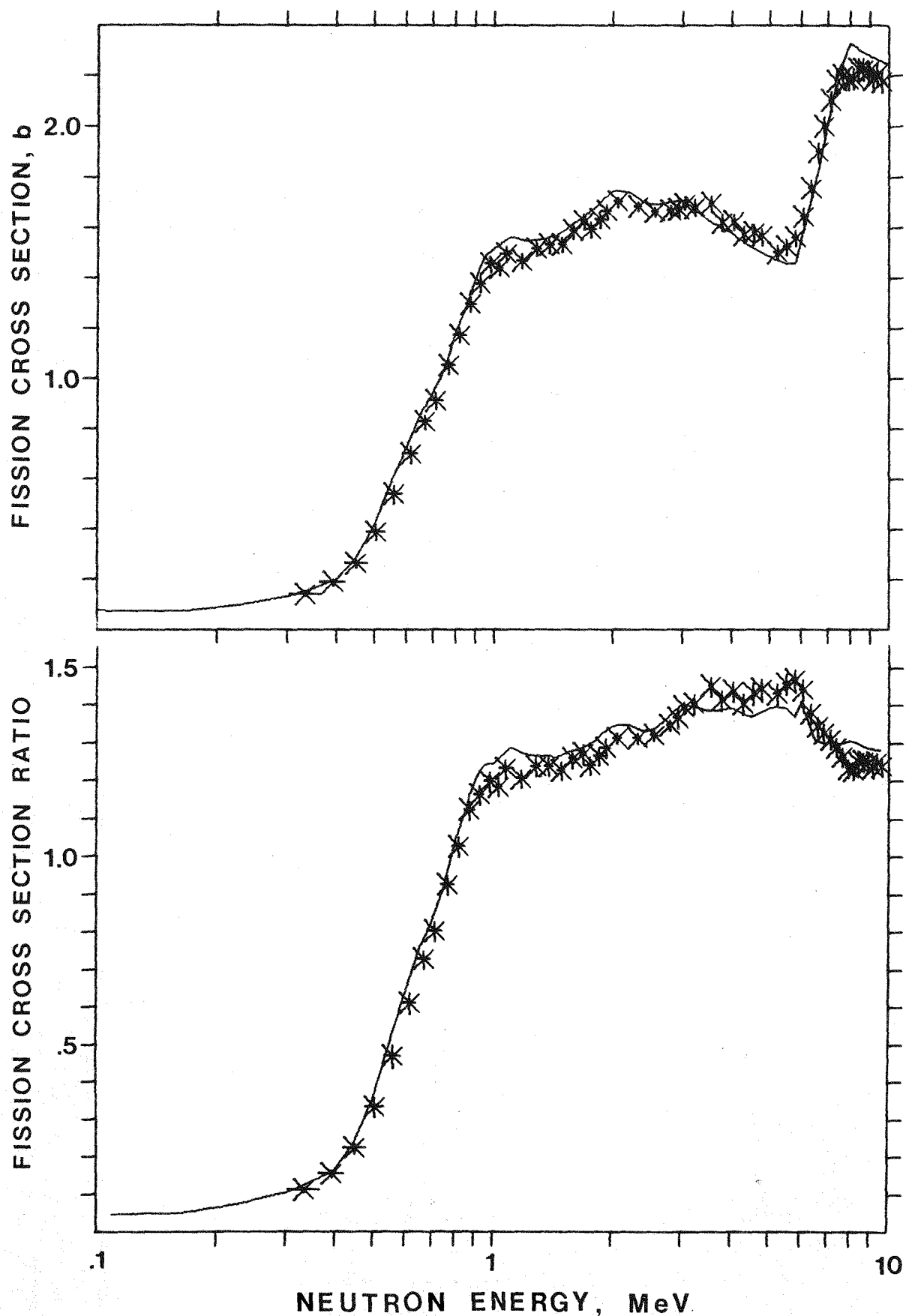


Fig. 11. The  $^{240}\text{Pu}/^{235}\text{U}$  fission cross section ratios and resultant  $^{240}\text{Pu}$  fission cross sections. The solid line is from ENDF/B-V.

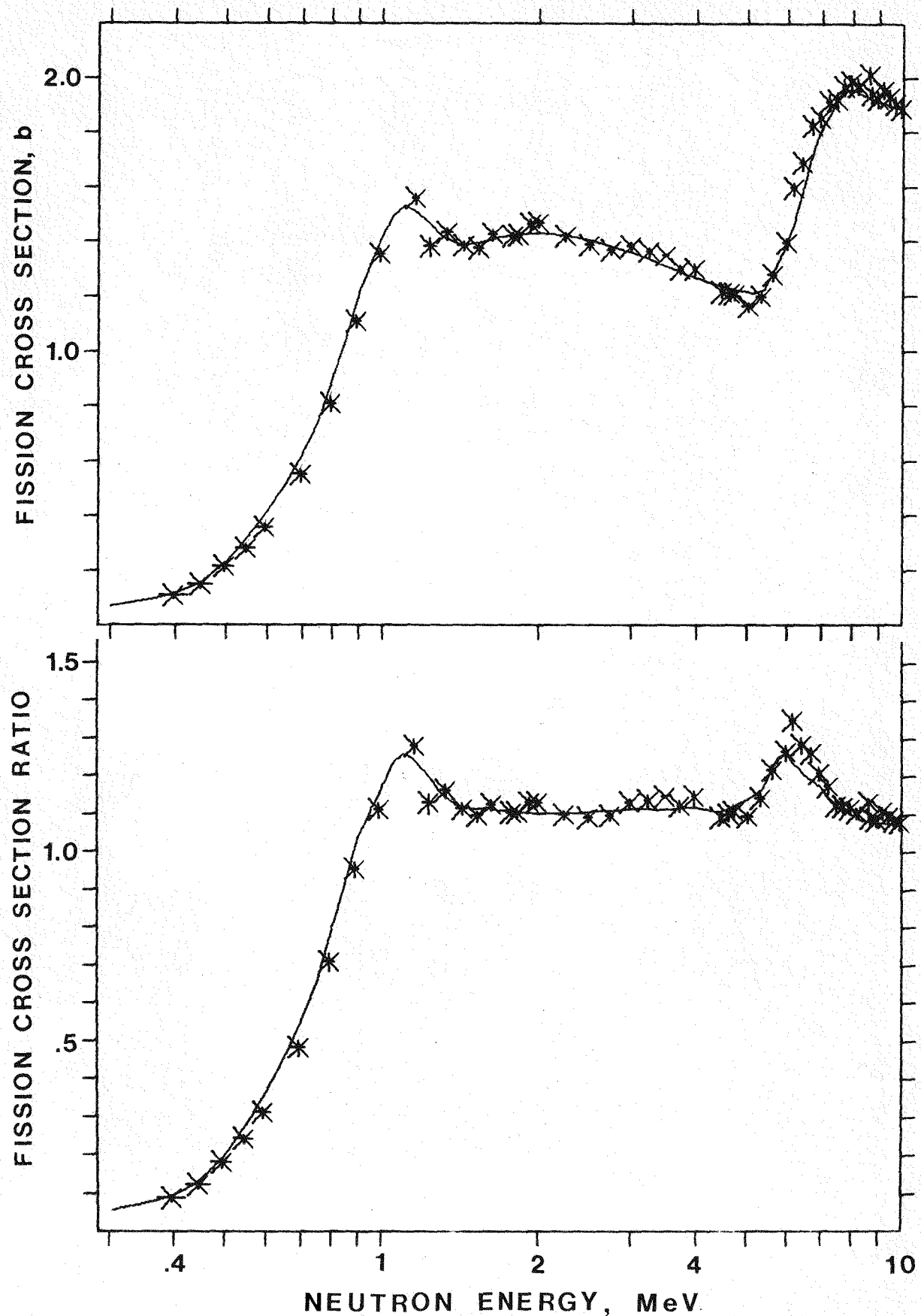


Fig. 12. The  $^{242}\text{Pu}/^{235}\text{U}$  fission cross section ratios and resultant  $^{242}\text{Pu}$  fission cross sections. The solid line is from ENDF/B-V.